Multiscale modeling and computation of flow through porous media

Yalchin Efendiev

Department of Mathematics

Texas A& M University

College Station, TX

Collaborators: T. Hou, V. Ginting, J. Aarnes, T. Strinopoulos

Two-phase flow model

- Viscous dominated (capillary effects are neglected)

$$-div(\lambda(S)k(x)\nabla p) = 0$$

$$S_t + v \cdot \nabla f(S) = 0, \quad v = -\lambda(S)k\nabla p.$$

- Flow and transport with capillary effects:

$$v = -\lambda(S)k(s)\nabla p_o + \lambda_w(S)\nabla p_c, \quad div(v) = 0$$

$$S_t + div(v_w) = 0.$$

Or

$$S_t + v \cdot \nabla f(S) = \nabla H(x, S)\nabla S$$

Homogenization of hyperbolic equations

- Hyperbolic equation with oscillatory periodic velocity field

$$\frac{\partial S^\epsilon}{\partial t} + v(x/\epsilon) \cdot \nabla S^\epsilon = 0.$$

- Homogenization depends on $(\overline{v}_1, \overline{v}_2) = \langle v(y) \rangle$.
- If $\overline{v}_1/\overline{v}_2$ is irrational number, the flow is ergodic and the homogenized equation is

$$\frac{\partial S}{\partial t} + \langle v \rangle \cdot \nabla S = 0.$$

- Otherwise, the flow can be reduced to layered flows

Layered flow

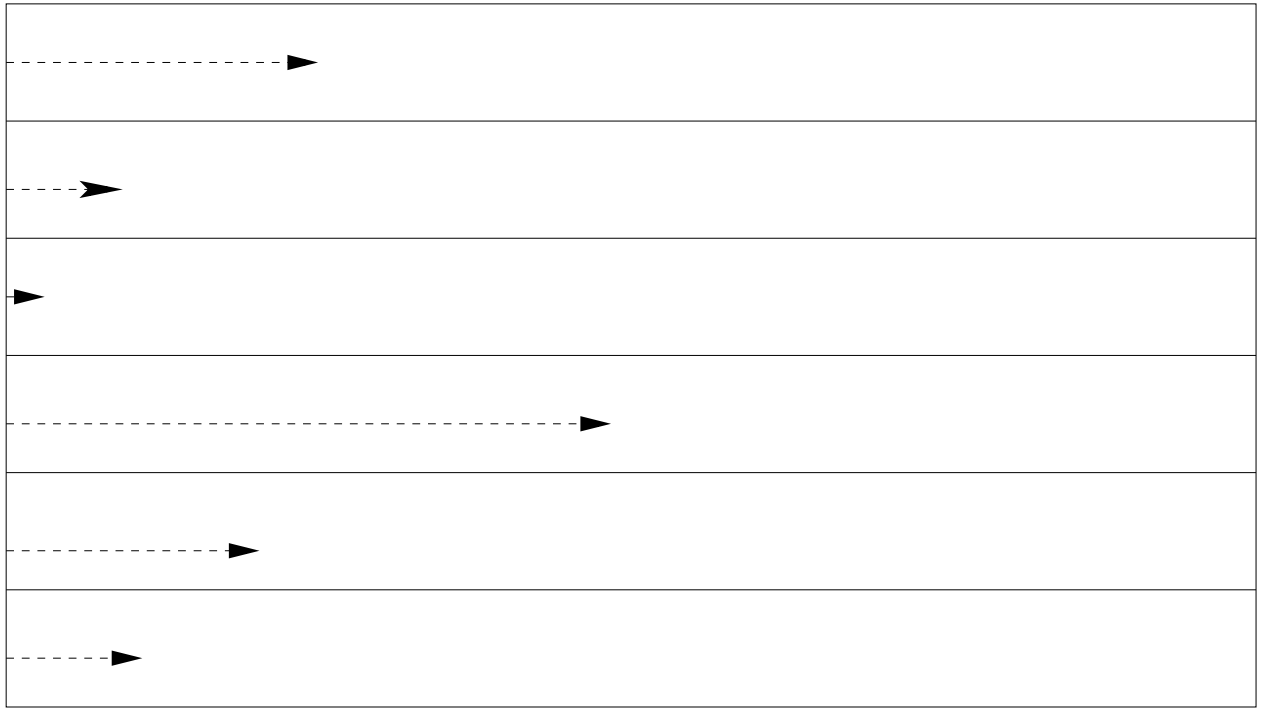

Homogenization of hyperbolic equations

- Hyperbolic equation with oscillatory velocity field

$$\frac{\partial S^\epsilon}{\partial t} + \mathbf{v}^\epsilon \cdot \nabla f(S^\epsilon) = 0$$

- Homogenized (macro-scale) equation is a non-local equation with memory effects.
- Consider the linear equation, $\frac{\partial S^\epsilon}{\partial t} + \mathbf{v}^\epsilon \cdot \nabla S^\epsilon = 0$, in a layered media, $\mathbf{v}^\epsilon = (v^\epsilon(y), 0)$.
- Assume the velocity $v^\epsilon(y)$ has finite number of distinct values v_i, $m_i = P\{v(y) = v_i\}$. Then the homogenized equation (Tartar, 89, Hou and Xin, 92)

$$\overline{S}_t + \overline{v}\overline{S}_x = \sum_k \int_0^t \beta_k \overline{S}_{xx}(x - u_k(t-\tau), \tau) d\tau.$$

Adding diffusion

- $$S_t^\epsilon + v(x/\epsilon) \cdot \nabla S^\epsilon = div(D \nabla S^\epsilon)$$

  Homogenized equation:

  $$S_t^\epsilon + \langle v \rangle \cdot \nabla S^\epsilon = div(D \nabla S^\epsilon)$$

- $$S_t^\epsilon + \frac{v(x/\epsilon)}{\epsilon} \cdot \nabla S^\epsilon = div(D \nabla S^\epsilon)$$

  $t^l_{con} = O(l/v)$, $t^l_{diff} = O(l^2/D)$.
  Homogenized equation:

  $$S_t^\epsilon + \frac{1}{\epsilon} \langle v \rangle \cdot \nabla S^\epsilon = div((D + q_{ij}) \nabla S^\epsilon)$$

- Enhanced diffusion ($\epsilon = 1$, $D = \delta$).

Two-phase flow effects

The effect of mobility.
Buckley-Leverett saturation profile.

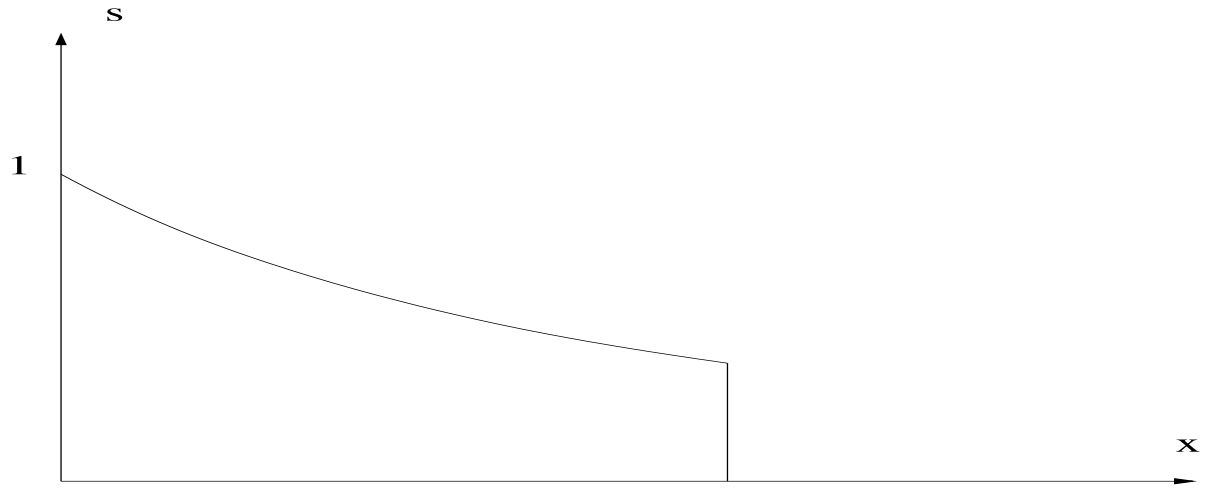

Assume homogeneous $k = 1$ and small front perturbation:

$$x(S_f, y, t) = u_0 f'(S_f)t + \frac{1}{2\pi}\int_{-\infty}^{\infty} \delta x_\alpha e^{i\alpha y} d\alpha.$$

Then, $\frac{d}{dt}\delta x_\alpha(t) = |\alpha|\frac{M_f - 1}{M_f + 1} u_0 f'(S_f)\delta x_\alpha(t)$, where $M_f = \lambda(S_f)/\lambda(0)$.

If small permeability variations are present

$$k = k_0 + \frac{1}{2\pi} \int_{-\infty}^{\infty} \delta k_\alpha(x) e^{i\alpha y} dy$$

then

$$\frac{d}{dt}\delta x_\alpha(t) = |\alpha| \frac{M_f - 1}{M_f + 1} u_0 f'(S_f) \delta x_\alpha(t) + \frac{\delta k_\alpha}{k_0}$$

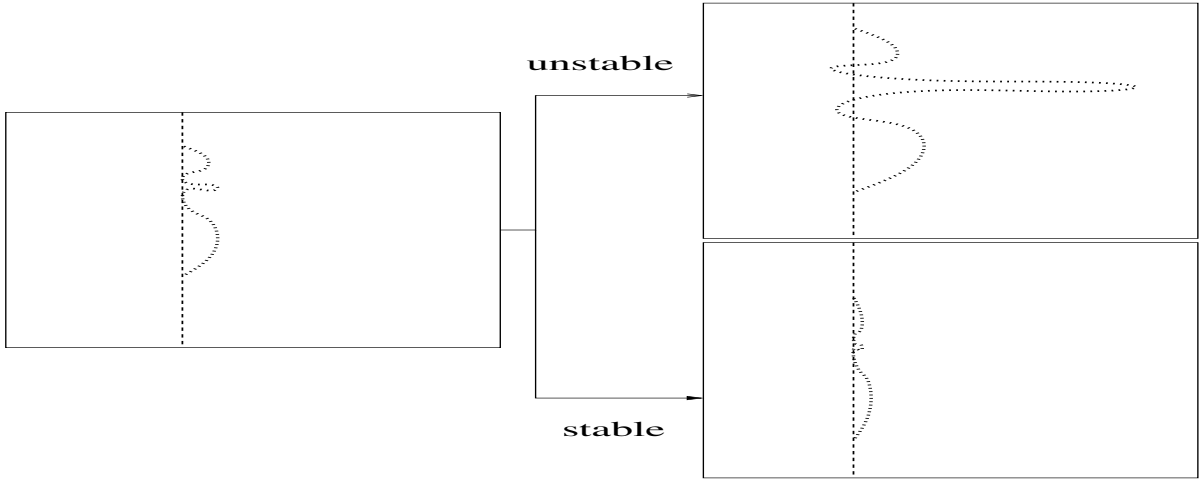

Homogenization of hyperbolic equations, continued

- Homogenization of nonlinear hyperbolic equations in layered media.
- Main idea: the use of piece-wise linear discretization of the flux and piece-wise constant discretization of the initial condition (Dafermos, 72).
- $\|S_k(\cdot,t) - S(\cdot,t)\|_{L_1} \leq \|S_k(\cdot,0) - S(\cdot,0)\|_{L_1} + Ct\|f_k - f\|_{Lip}$.
- Homogenized equation (Efendiev and Popov, 2005)

$$\overline{S}_t + U\overline{S}_x = \sum_{k=1} \int_0^t \beta_k \overline{S}_{xx}(x - u_k(t-\tau), \tau) d\tau,$$

where β_k and u_k depend only on one point correlations of v, $f'(S)$ and are defined from (Riemann problem)

$$\sum_k \frac{\beta_k}{u_k - z} = \left(\sum_{i,j} \frac{m_i \Delta_j}{z - v_i f'(S_j)} \right)^{-1} - z + U, \quad \forall z \in C.$$

Perturbation technique

- Consider

$$\frac{\partial S^\epsilon}{\partial t} + \mathbf{v}^\epsilon \cdot \nabla S^\epsilon = 0$$

  Expand the velocity and the saturation

$$\mathbf{v}_\epsilon = \overline{\mathbf{v}} + \mathbf{v}', \quad S^\epsilon = \overline{S} + S^{'}$$

- The fluctuations can be neglected on the scale of a coarse grid block (not on the scale of the entire domain!).
- Substituting the expansion into the equation and taking “average”

$$\frac{\partial \overline{S}}{\partial t} + \overline{\mathbf{v}} \cdot \nabla \overline{S} + \overline{\mathbf{v}' \cdot \nabla S'} = 0.$$

  Here we have used $\overline{S'} = 0$, $\overline{\mathbf{v}'} = 0$.

Perturbation technique, continued

- $\overline{\mathbf{v}^{'} \cdot \nabla S^{'}}$ represent the macro scale effects associated with the small scales. To approximate it the equation for the fluctuating components is used

$$\frac{\partial S^{'}}{\partial t} + \overline{\mathbf{v}} \cdot \nabla S^{'} + \mathbf{v}^{'} \cdot \nabla \overline{S} + \mathbf{v}^{'} \cdot \nabla S^{'} = \overline{\mathbf{v}^{'} \cdot \nabla S^{'}}.$$

- Solving for $S^{'}$ along the streamline $d\mathbf{x}/dt = \overline{\mathbf{v}}$ we get

$$v_k^{'} S^{'} = - \int_0^t v_k^{'}(\mathbf{x}) v_j^{'}(\mathbf{x}(\tau)) \nabla_j \overline{S} d\tau + H.O.T$$

  - Then $\overline{\mathbf{v}^{'} S^{'}}$ is given by

$$\overline{v_k^{'} S^{'}} = - \int_0^t \overline{v_k^{'}(x) v_j^{'}(x(\tau))} d\tau \nabla_j \overline{S}$$

Perturbation technique, continued

- The coarse scale equation is (Efendiev et al., WRR, 2000)

$$\frac{\partial \overline{S}}{\partial t} + \overline{v} \cdot \nabla \overline{S} = \nabla_i D^{ij} \nabla_j \overline{S},$$

  where $D^{ij} = \int_0^t \overline{v_j'(\mathbf{x}) v_k'(\mathbf{x}(\tau))} d\tau$

- The correlation of the velocity appears as a diffusivity

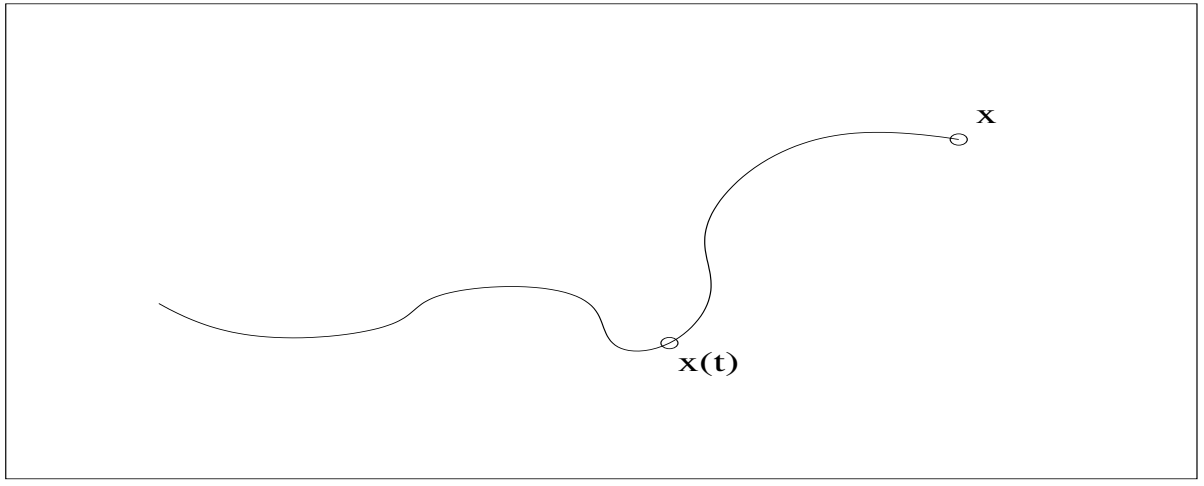

Perturbation technique for nonlinear saturation equation

- The approximate macro scale equation is (Efendiev et al., WRR, 2002)

$$\frac{\partial \overline{S}}{\partial t} + \overline{\mathbf{v}} \cdot \nabla f(\overline{S}) = \nabla_i f'(\overline{S})^2 D^{ij} \nabla_j \overline{S}$$

- D^{ij} depends on two point correlation of the velocity field and $\overline{S}$.
- The overall approach is obtained by combining the saturation equation with the pressure equation in the form $\nabla \cdot \lambda(\overline{S}) \mathbf{k} \nabla p = 0$.
- The multiscale base functions are constructed once. The two-point correlation of the velocity can be found using the multiscale base functions. This approach is very efficient and can predict the quantity of interest on a highly coarsened grid.

The essence of the derivation

- Expand $\mathbf{v}_\epsilon = \overline{\mathbf{v}} + \mathbf{v}'$, $S^\epsilon = \overline{S} + S'$, and $f = \overline{f} + f'$. Substitute the expansions into the original equation and take average

$$\frac{\partial \overline{S}}{\partial t} + \overline{\mathbf{v}} \cdot \nabla f(\overline{S}) + \overline{\nabla \cdot f_S(\overline{S}) \mathbf{v}' S'} + \frac{1}{2} \nabla \cdot \overline{\mathbf{v}} f_{SS}(\overline{S}) \overline{S'^2} = 0.$$

- We need to model the coarse scale quantities, velocity-saturation covariance ($\overline{\mathbf{v}' S'}$), and saturation-saturation covariance ($\overline{S' S'}$). Their modeling is based on the equation for fluctuating components

$$\frac{\partial S'}{\partial t} + \overline{v}_j S' f_{SS}(\overline{S}) \nabla_j \overline{S} + \overline{v}_j f_S(\overline{S}) \nabla_j S' + v_j' f_S(\overline{S}) \nabla_j \overline{S} = \Phi(\mathbf{x}, t),$$

where $\Phi(\mathbf{x}, t)$ is a coarse scale function.

The essence of the derivation, continued

- Solving for S' along the coarse trajectories $d\mathbf{x}/dt = \overline{\mathbf{v}} f_S(\overline{S})$,

$$S^{'}(\mathbf{x},t) = \int_0^t -v_j^{'}(\mathbf{x}(\tau),\tau) f_S(\overline{S}(\tau,\mathbf{x}(\tau)))\nabla_j \overline{S}(\tau,\mathbf{x}(\tau)) \exp\,(-\int_\tau^t L(\mathbf{x}(\mu),\mu)d\mu\,)d\tau,$$

  where $L(\mathbf{x}(\mu),\mu)$ is a coarse scale function. From here $\overline{\mathbf{v}'(\mathbf{x},t)S'(\mathbf{x},t)}$ and $\overline{S'(\mathbf{x},t)S'(\mathbf{x},t)}$ can be evaluated.

- Further we simplify the expression showing that $d\overline{S}(\mathbf{x}(t),t)/dt = O(v'^2)$, if $f'(0) = f'(1) = 0$.

Nonlinear equation

• We propose an alternative way to calculate the diagonal components of two-point correlation of the velocity

$$v_i^{'}(\mathbf{x},t)v_i^{'}(\mathbf{x}(\tau),\tau) \approx \alpha(\sigma,l_x,l_z)\mathrm{std}(v_i(\mathbf{x},t))\overline{v}_i(\mathbf{x}(\tau),\tau).$$

Coarse grid equation in FV framework

- Coarse grid transport equation:

$$\frac{\partial \overline{S}}{\partial t} + \overline{v} \cdot \nabla \overline{S} = \nabla \cdot \left\{ D(x,t) \nabla \overline{S}(x,t) \right\} \qquad \text{(single-phase)},$$

$$\frac{\partial \overline{S}}{\partial t} + \overline{v} \cdot \nabla f(\overline{S}) = \nabla \cdot \left\{ f_S(\overline{S})^2 \, D(x,t) \nabla \overline{S}(x,t) \right\} \qquad \text{(multi-phase)}$$

  where

$$D_{ij}(x,t) = \int_{V_x\, i} \left[\int_0^t v_i'(x) v_j'(x(\tau)) d\tau \right] dA.$$

- First order approximation: $D_{ij}(x,t) = \int_{V_x\, i} v_i'(x) L_j dA$,

Numerical Results. Exponential variogram

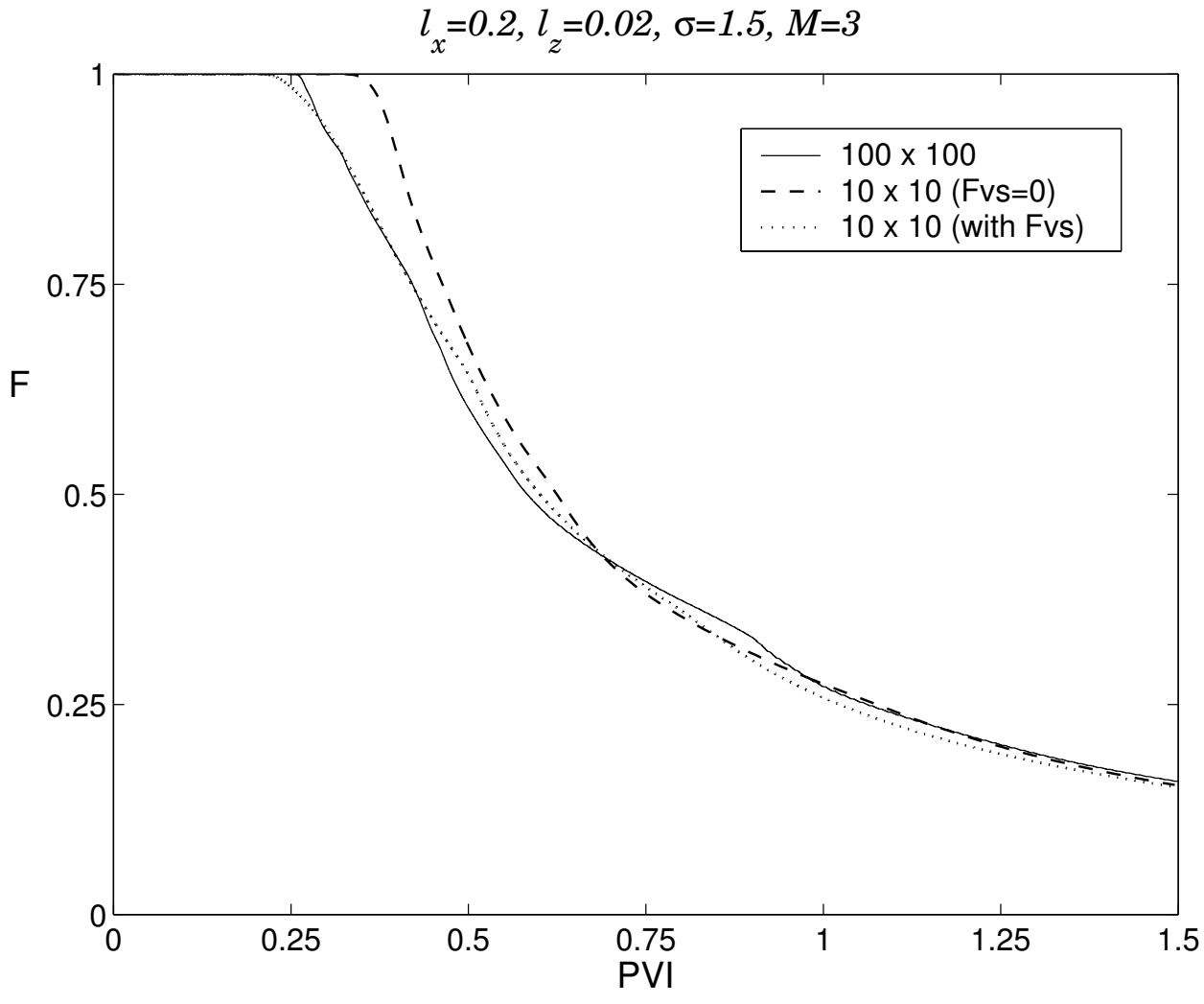

Numerical Results. Exponential variogram

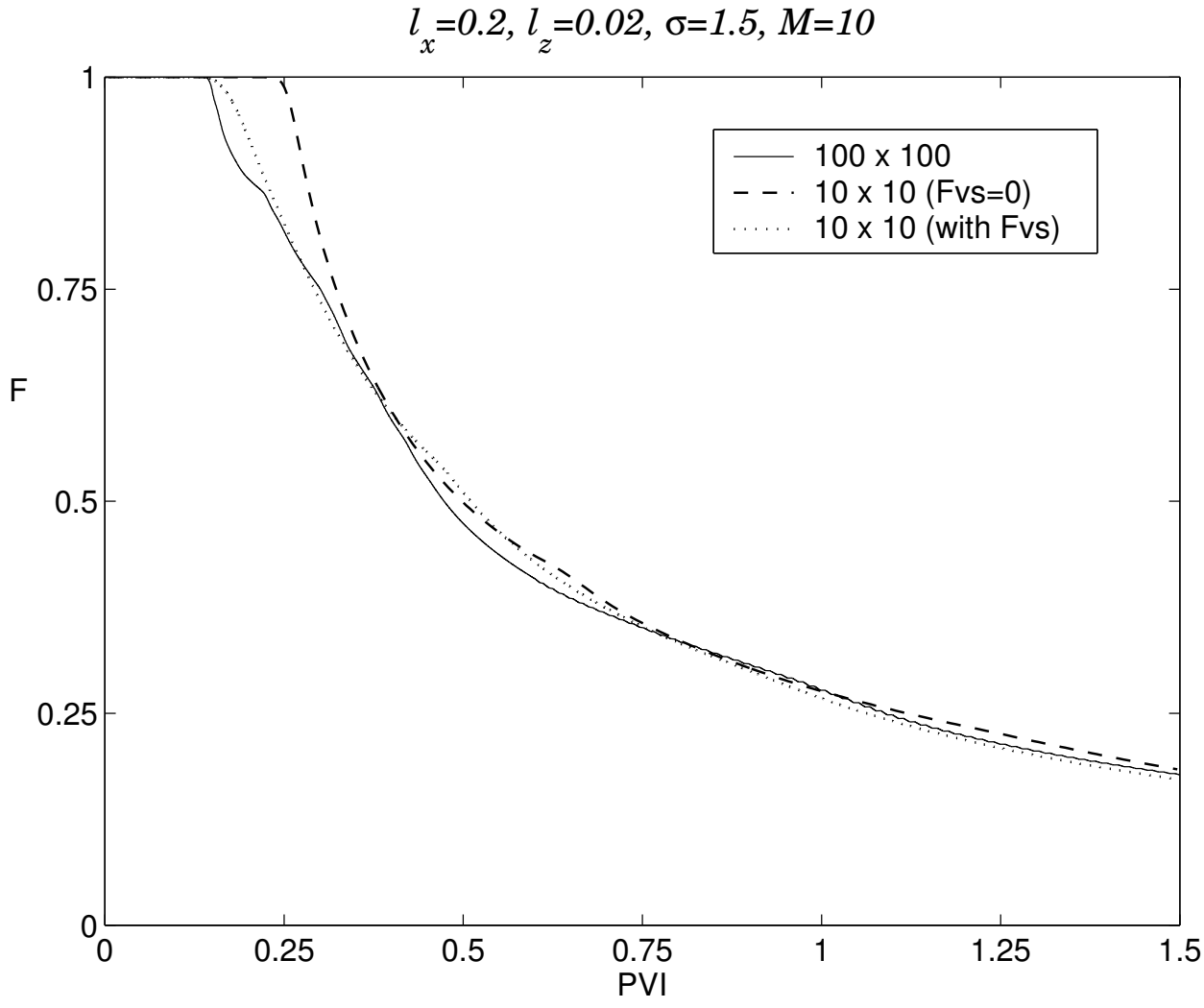

Numerical Results. Spherical variogram

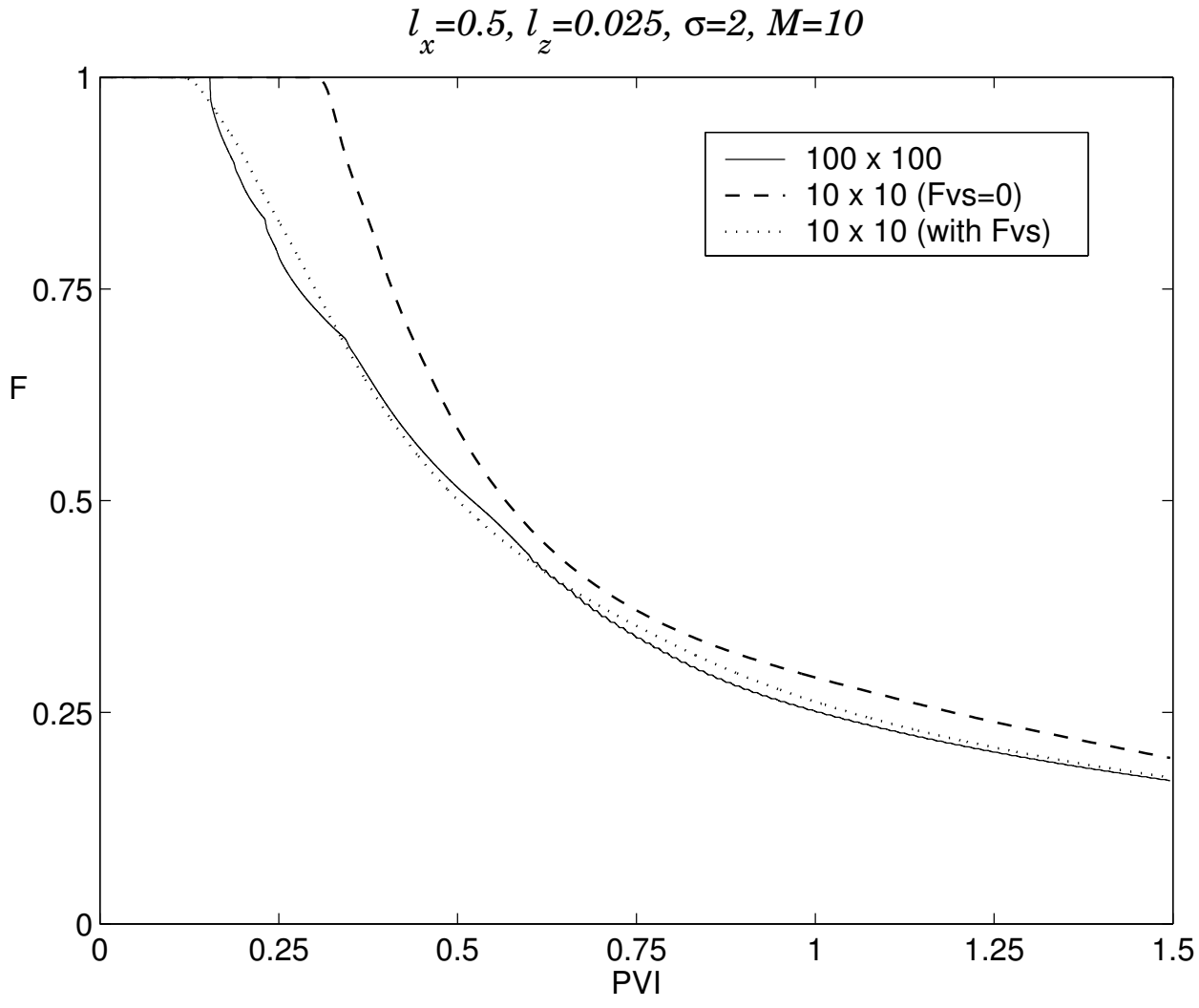

Numerical Results. Spherical variogram

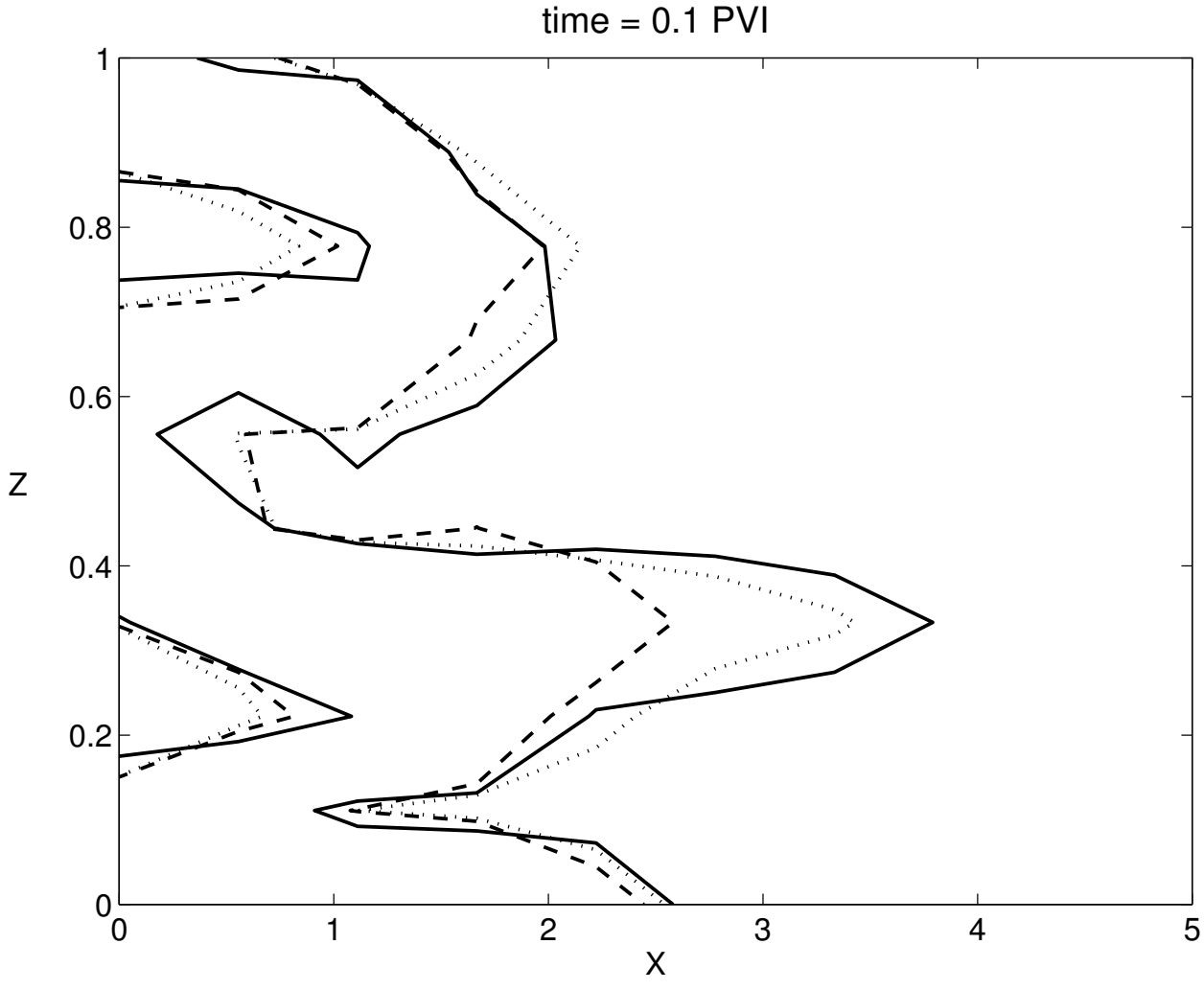

Numerical Results. Spherical variogram

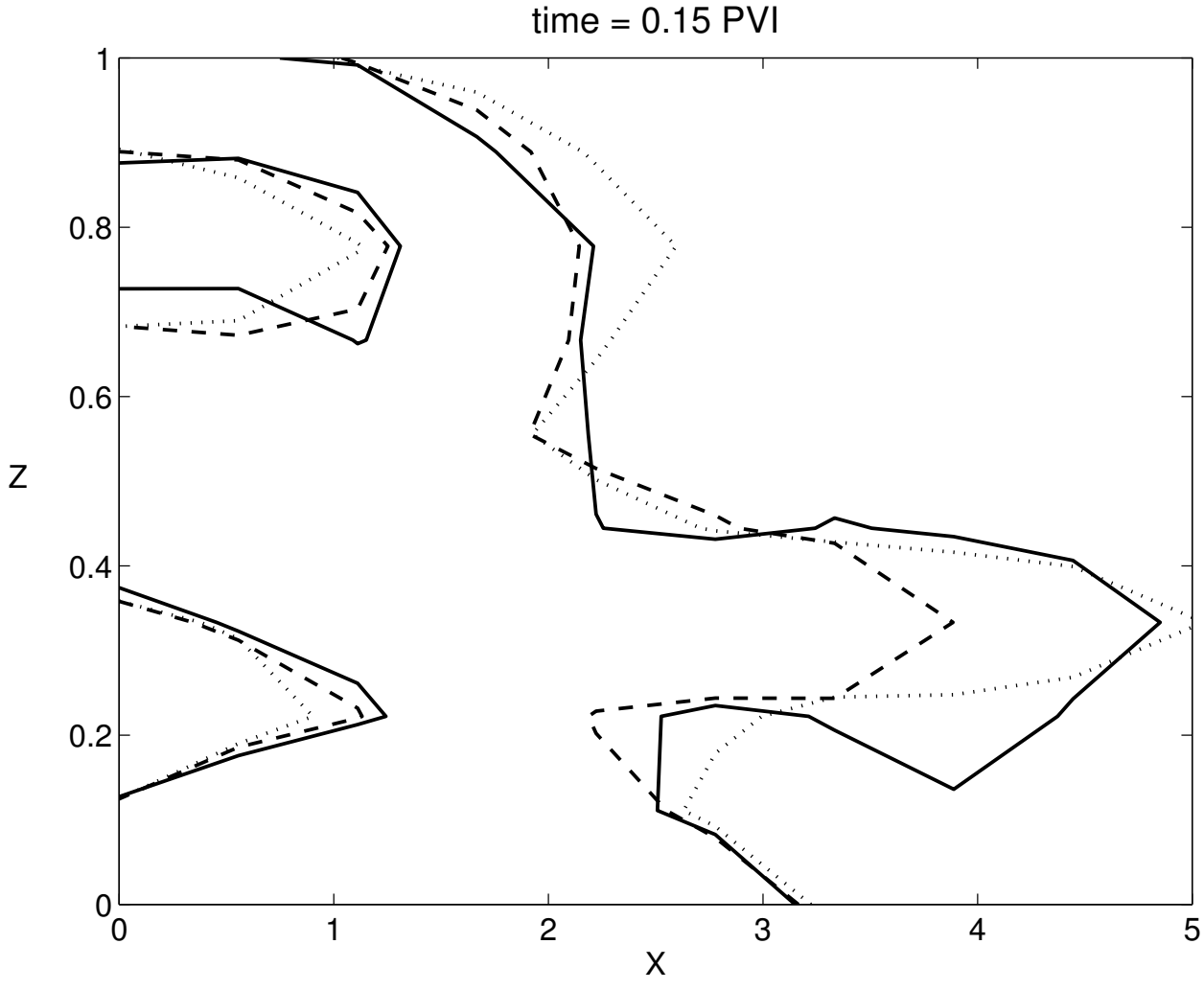

Two-component miscible flow

- $$-\nabla \cdot \left\{ \frac{k(x)}{\mu(C)} \nabla p \right\} = q$$
$$\frac{\partial C}{\partial t} + v \cdot \nabla C = (\tilde{C} - C)q.$$
- $$\mu(C) = \frac{\mu(0)}{\left(1 - C + M^{\frac{1}{4}} C\right)^4},$$
- The pressure equation is solved using the MsFVEM.

Existing upscaling techniques

- $-div(\lambda(S)k\nabla p) = 0$, $S_t + v \cdot \nabla f(S) = 0$, $v = -\lambda(S)k\nabla p$.
- Single-phase upscaling: $(k \longrightarrow k^*)$, $\mathbf{k}^* = \frac{\overline{\mathbf{k}\nabla p}}{\overline{\nabla p}}$.

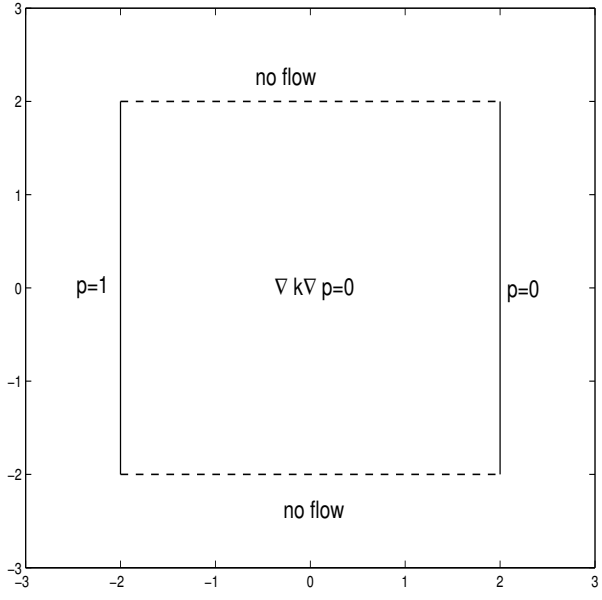

- Multiphase upscaling $\lambda \longrightarrow \lambda^*$, $f \longrightarrow f^*$.

Multiscale methods for two-phase flow in flow-based coordinate system

Two-phase flow equations in flow-based coor.

$$\frac{\partial}{\partial \psi}\left(k^2\lambda(S)\frac{\partial P}{\partial \psi}\right)+\frac{\partial}{\partial p}\left(\lambda(S)\frac{\partial P}{\partial p}\right)=0.$$

$$\frac{\partial S}{\partial t}+(\mathbf{v}\cdot\nabla\psi)\frac{\partial f(S)}{\partial \psi}+(\mathbf{v}\cdot\nabla p)\frac{\partial f(S)}{\partial p}=0.$$

Consider $\lambda(S)=1$. Homogenization of hyperbolic equations.

$$\begin{aligned} S_t^\epsilon + v_0^\epsilon f(S^\epsilon)_p &= 0 \\ S(p,\psi,t=0) &= S_0, \end{aligned}$$

$$v_0^\epsilon(p)=v_0(p,\frac{p}{\epsilon}).$$

Homogenization of transport

Then, for each ψ, it can be shown that $S^\epsilon(p,\psi,t) \to \tilde{S}(p,\psi,t)$ in $L^1((0,1)\times(0,T))$, where $\tilde{S}$ satisfies

$$\tilde{S}_t + \tilde{v}_0 f(\tilde{S})_p = 0,$$

where $\tilde{v}_0$ is harmonic average of v_0^ϵ, i.e.,

$$\frac{1}{v_0^\epsilon} \to \frac{1}{\tilde{v}_0} \quad \text{weak} * \text{ in } L^\infty(0,1).$$

Proof: (1) use of two-scale Young measures OR (2) one can follow Bourgeat and Mikelic's work.

Theorem.

$$\|S^\epsilon - \tilde{S}\|_n \le G\epsilon^{1/n}.$$

Note. $\tilde{S}$ can be considered as an upscaled S^ϵ along streamlines. Can we average across streamlines?

Homogenization across streamlines

If the velocity field does not depend on p inside the cells, that is, $\tilde{v}(\psi, \frac{\psi}{\epsilon})$, then the homogenized solution, $\overline{\tilde{S}}$, (weak* limit of $\tilde{S}$, which will be denoted by $\overline{S}$), satisfies

$$\overline{S}_t + \overline{\tilde{v}}_0 \overline{S}_p = \int_0^t \int \overline{S}_{pp}(p - \lambda(t-\tau), \psi, \tau) d\mu_{\frac{\psi}{\epsilon}}(\lambda) d\tau.$$

Here, $d\nu_{\frac{\psi}{\epsilon}}$ the Young measure associated with the sequence $\tilde{v}_0(\psi, \cdot)$ and $d\mu_{\frac{\psi}{\epsilon}}$ is a Young measure that satisfies

$$\left(\int \frac{d\nu_{\frac{\psi}{\epsilon}}(\lambda)}{\frac{s}{2\pi i q} + \lambda} \right)^{-1} = \frac{s}{2\pi i q} + \overline{\tilde{v}}_0 - \int \frac{d\mu_{\frac{\psi}{\epsilon}}(\lambda)}{\frac{s}{2\pi i q} + \lambda}.$$

We have denoted by $\overline{\tilde{v}}_0$ the weak limit of the velocity. This equation has no dependence on the small scale and we consider it to be the full homogenization of the fine saturation equation.
We have extended this method for the Riemann problem in the case of nonlinear flux.

Numerical Averaging across Streamlines

$$\tilde{S} = \overline{S}(p, \psi, t) + S'(p, \psi, \zeta, t)$$

$$\tilde{v}_0 = \overline{\tilde{v}_0}(p, \psi, t) + \tilde{v}_0'(p, \psi, \zeta, t).$$

First, consider $f(S) = S$. Averaging fine-scale equations with respect to ψ we find an equation for the mean of the saturation

$$\overline{S}_t + \overline{\tilde{v}_0 \overline{S}_p} + \overline{\tilde{v}_0' S_p'} = 0.$$

An equation for the fluctuations is

$$S_t' + (\tilde{v}_0 - \overline{\tilde{v}_0})\overline{S}_p + \tilde{v}_0 S_p' - \overline{\tilde{v}_0' S_p'} = 0.$$

Together, the equations for the saturation are

$$\begin{aligned} \overline{S}_t + \overline{\tilde{v}_0 \overline{S}_p} + \overline{\tilde{v}_0' S_p'} &= 0 \\ S_t' + \tilde{v}_0' \overline{S}_p + \tilde{v}_0 S_p' - \overline{\tilde{v}_0' S_p'} &= 0. \end{aligned} \tag{1}$$

$$\frac{dP}{dt} = \overline{\tilde{v}_0}, \text{ with } P(p,0) = p.$$

$$S' = -\int_0^t \left(\tilde{v}_0'(P(p,\tau),\psi)\overline{S}_p(P(p,\tau),\psi,\tau) + \tilde{v}_0'(P(p,\tau),\psi)S_p'(P(p,\tau),\psi,\tau) + \overline{\tilde{v}_0' S_p'} \right) d\tau.$$

$$\frac{dP}{dt} = \overline{\tilde{v}_0}, \text{ with } P(p,0) = p.$$

$$S' = -\int_0^t \left(\tilde{v}_0'(P(p,\tau),\psi)\overline{S}_p(P(p,\tau),\psi,\tau) + \tilde{v}_0'(P(p,\tau),\psi)S_p'(P(p,\tau),\psi,\tau) + \overline{\tilde{v}_0' S_p'} \right) d\tau.$$

$$\overline{\tilde{v}_0' S'} = -\int_0^t \overline{\tilde{v}_0' \tilde{v}_0(P(p,\tau),\psi)\overline{S}_p(P(p,\tau),\psi,\tau)} d\tau.$$

It can be easily shown that $\overline{S}_p(P(p,\tau)$ depends weakly on time. Then

$$\overline{\tilde{v}_0' S'} = -\int_0^t \overline{\tilde{v}_0' \tilde{v}_0'(P(p,\tau),\psi)} d\tau \overline{S}_p.$$

Nonlinear case

$$\begin{aligned} \overline{S}_t + \overline{\tilde{v}_0} f(\overline{S})_p + \overline{\tilde{v}_0'(f_S(\overline{S})S')_p} &= 0 \\ S_t' + \tilde{v}_0' f_S(\overline{S})\overline{S}_p + \tilde{v}_0 f_S(\overline{S})S_p' - \overline{\tilde{v}_0' S_p'} &= 0. \end{aligned}$$

The macrodispersion is discretized as

$$\overline{\tilde{v}_0'(f_S(\overline{S})S')_p} = \frac{\overline{\tilde{v}_0' f_S(\overline{S})S'}^{i+1} - \overline{\tilde{v}_0' f_S(\overline{S})S'}^{i}}{\Delta p} + O(\Delta p).$$

We solve the second equation on the coarse characteristics defined by

$$\frac{dP}{dt} = \overline{\tilde{v}_0} f_S(\overline{S}), \text{ with } P(p,0) = p$$

and form the terms that appear in the macrodispersion

$$\overline{\tilde{v}_0' f_S(\overline{S})S'} = -\int_0^t \overline{\tilde{v}_0' f_S(\overline{S})\tilde{v}_0'(P(p,\tau),\psi) f_S(\overline{S}(P(p,\tau),\psi,\tau))\overline{S}_p(P(p,\tau),\psi,\tau)}d\tau.$$

Nonlinear case

We have dropped terms that are second-order in fluctuating quantities. It can be shown that $f_S(\overline{S}(P(p,\tau),\psi,\tau))\overline{S}_p(P(p,\tau),\psi,\tau)$ does not vary significantly along the streamlines and it can be taken out of the integration in time:

$$\overline{\tilde{v}_0' f_S(\overline{S}) S'} = -\int_0^t \overline{\tilde{v}_0' \tilde{v}_0'(P(p,\tau),\psi)} d\tau f_S(\overline{S})^2 \overline{S}_p.$$

This expression is similar to the one obtained in the linear case, however the macrodispersion depends on the past saturation through the equation for the coarse characteristics.

Numerical results

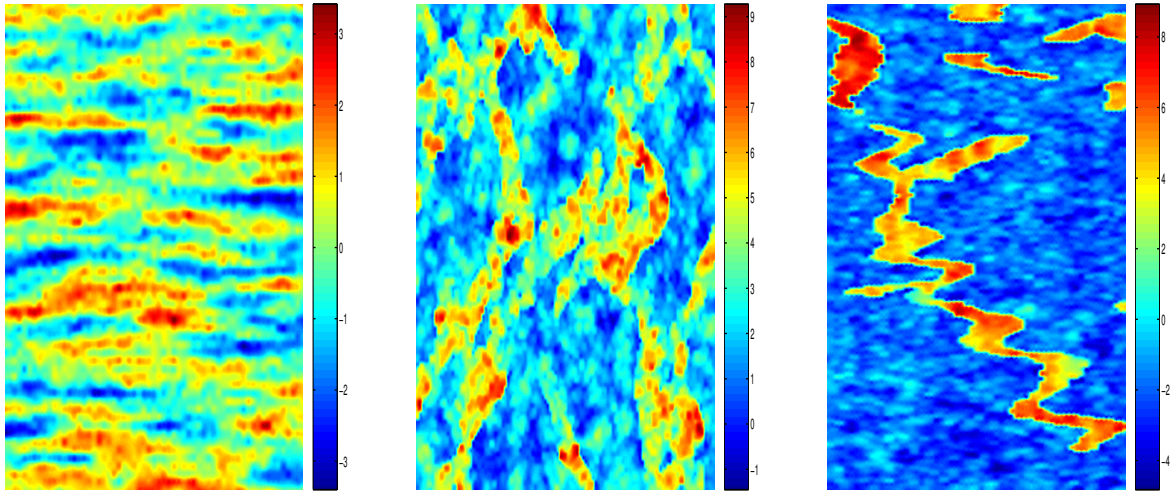

Permeability fields used in the simulations. Left - permeability field with exponential variogram, middle - synthetic channelized permeability field, right - layer 36 of SPE comparative project

Numerical results

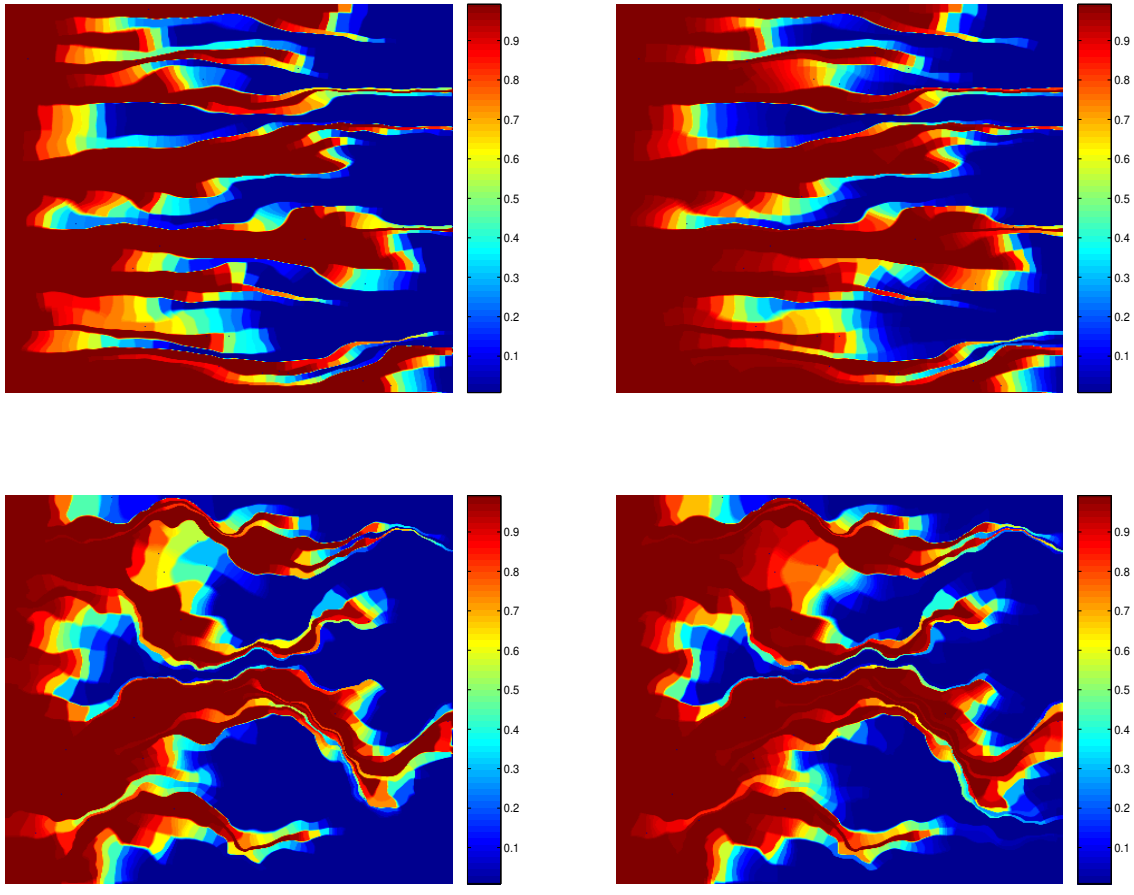

Saturation snapshots for variogram based permeability field (top) and synthetic channelized permeability field (bottom). Linear flux is used. Left figures represent the upscaled saturation plots and the right figures represent the fine-scale saturation plots.

Numerical results

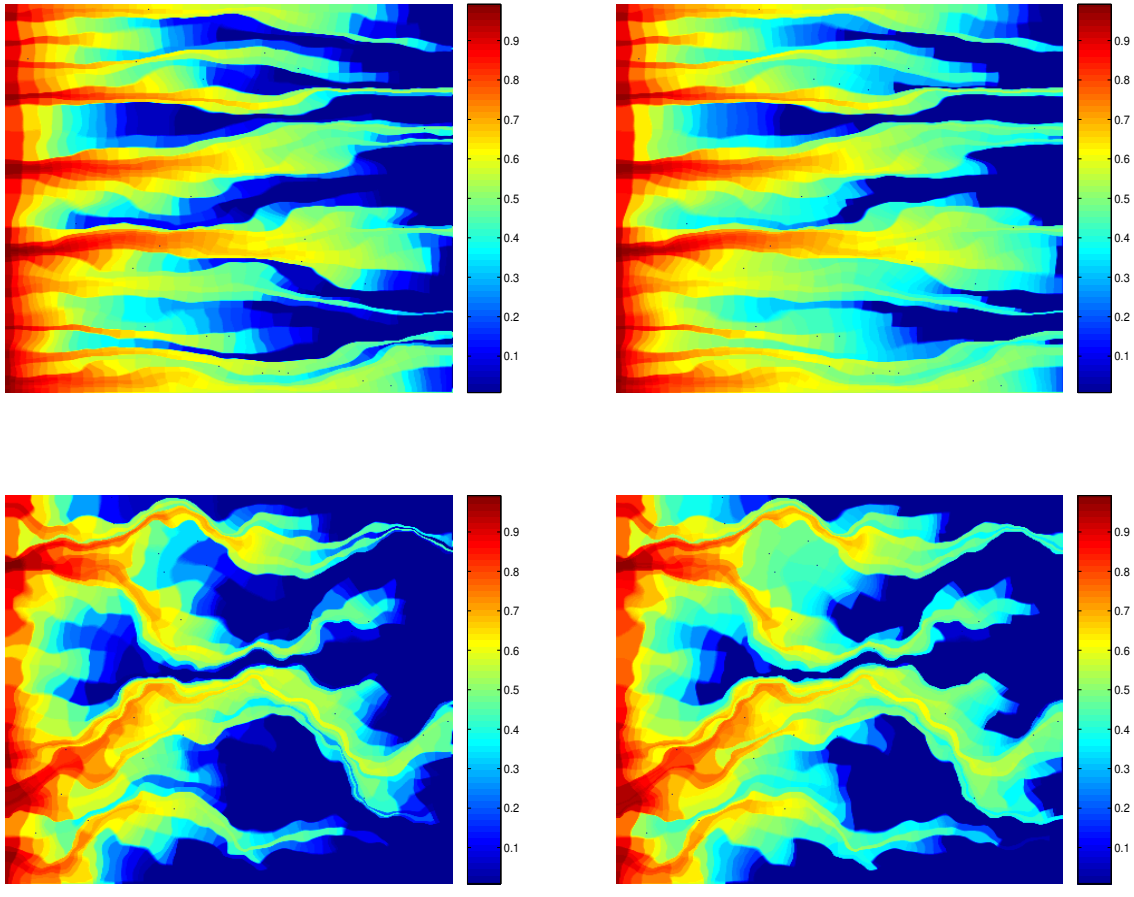

Saturation snapshots for variogram based permeability field (top) and synthetic channelized permeability field (bottom). Nonlinear flux is used. Left figures represent the upscaled saturation plots and the right figures represent the fine-scale saturation plots.

Numerical results

Upscaling error for permeability generated using two-point geostatistics

LINEAR FLUX	25x25	50x50	100x100	200x200
L_1 error of $\tilde{S}$	0.0021	$6.57e-4$	$2.15e-4$	$8.75e-5$
L_1 error of $\overline{S}$ with macrodispersion	0.115	0.0696	0.0364	0.0135
L_1 error of $\overline{S}$ fine without macrodispersion	0.1843	0.0997	0.0505	0.0191

NONLINEAR FLUX	25x25	50x50	100x100	200x200
L_1 error of $\tilde{S}$	0.0023	$8.05e-4$	$2.89e-4$	$1.29e-4$
L_1 error of $\overline{S}$ with macrodispersion	0.116	0.0665	0.0433	0.0177
L_1 error of $\overline{S}$ fine without macrodispersion	0.151	0.0805	0.0432	0.0186

Numerical results

Upscaling error for for synthetic channelized permeability field

LINEAR FLUX	25x25	50x50	100x100	200x200
L_1 error of $\tilde{S}$	0.0222	0.0171	0.0122	0.0053
L_1 error of $\overline{S}$ with macrodispersion	0.0819	0.0534	0.0333	0.0178
L_1 error of $\overline{S}$ fine without macrodispersion	0.123	0.0834	0.0486	0.0209
NONLINEAR FLUX	25x25	50x50	100x100	200x200
L_1 error of $\tilde{S}$	0.0147	0.0105	0.0075	0.0040
L_1 error of $\overline{S}$ with macrodispersion	0.0842	0.0658	0.0371	0.0207
L_1 error of $\overline{S}$ fine without macrodispersion	0.119	0.0744	0.0424	0.0214

Numerical results

Upscaling error for SPE 10, layer 36

LINEAR FLUX	25x25	50x50	100x100	200x200
L_1 error of $\tilde{S}$	0.0128	0.0093	0.0072	0.0042
L_1 error of $\overline{S}$ with macrodispersion	0.0554	0.0435	0.0307	0.0176
L_1 error of $\overline{S}$ fine without macrodispersion	0.123	0.0798	0.0484	0.0258

NONLINEAR FLUX	25x25	50x50	100x100	200x200
L_1 error of $\tilde{S}$	0.0089	0.0064	0.0054	0.0033
L_1 error of $\overline{S}$ with macrodispersion	0.0743	0.0538	0.0348	0.0189
L_1 error of $\overline{S}$ fine without macrodispersion	0.0924	0.0602	0.0395	0.0202

Numerical results

Total error for permeability field generated using two-point geostatistics

LINEAR FLUX	25x25	50x50	100x100	200x200
L_1 upscaling error of $\tilde{S}$	0.0021	$6.57e-4$	$2.15e-4$	$8.75e-5$
L_1 error of $\tilde{S}$ computed on coarse grid	0.0185	0.0062	0.0019	0.0015
L_1 upscaling error of $\overline{S}$	0.115	0.0696	0.0364	0.0135
L_1 error of computed on coarse grid	0.139	0.0779	0.0390	0.0144

NONLINEAR FLUX	25x25	50x50	100x100	200x200
L_1 upscaling error of $\tilde{S}$	0.0023	$8.05e-4$	$2.89e-4$	$1.29e-4$
L_1 error of $\tilde{S}$ computed on coarse grid	0.0268	0.0099	0.0027	$9.38e-4$
L_1 upscaling error of $\overline{S}$	0.116	0.0665	0.0433	0.0177
L_1 error of $\overline{S}$ computed on coarse grid	0.146	0.0797	0.0461	0.0184

Numerical results

Total error for synthetic channelized permeability field

LINEAR FLUX	25x25	50x50	100x100	200x200
L_1 upscaling error of $\tilde{S}$	0.0222	0.0171	0.0122	0.0053
L_1 error of $\tilde{S}$ computed on coarse grid	0.0326	0.0161	0.0107	0.0113
L_1 upscaling error of $\overline{S}$	0.0819	0.0534	0.0333	0.0178
L_1 error of $\overline{S}$ computed on coarse grid	0.135	0.0849	0.0477	0.0274

NONLINEAR FLUX	25x25	50x50	100x100	200x200
L_1 upscaling error of $\tilde{S}$	0.0147	0.0105	0.0075	0.0040
L_1 error of $\tilde{S}$ computed on coarse grid	0.0494	0.0295	0.0150	0.0130
L_1 upscaling error of $\overline{S}$	0.0842	0.0658	0.0371	0.0207
L_1 error of $\overline{S}$ computed on coarse grid	0.17	0.11	0.0541	0.0303

Numerical results

Total error for SPE10 layer 36

LINEAR FLUX	25x25	50x50	100x100	200x200
L_1 upscaling error of $\tilde{S}$	0.0128	0.0093	0.0072	0.0042
L_1 error of $\tilde{S}$ computed on coarse grid	0.023	0.0095	0.0069	0.0052
L_1 upscaling error of $\overline{S}$	0.0554	0.0435	0.0307	0.0176
L_1 error of $\overline{S}$ computed on coarse grid	0.0683	0.052	0.0361	0.0205

NONLINEAR FLUX	25x25	50x50	100x100	200x200
L_1 upscaling error of $\tilde{S}$	0.0089	0.0064	0.0054	0.0033
L_1 error of $\tilde{S}$ computed on coarse grid	0.0338	0.0148	0.0074	0.0037
L_1 upscaling error of $\overline{S}$	0.0743	0.0538	0.0348	0.0189
L_1 error of $\overline{S}$ computed on coarse grid	0.115	0.0720	0.0406	0.0204

Numerical results

Computational cost

	fine $x.y$	fine p, ψ	$\tilde{S}$	$\overline{S}$
layered, linear flux	5648	257	9	1
layered, nonlinear flux	14543	945	28	4
percolation, linear flux	8812	552	12	1
percolation, nonlinear flux	23466	579	12	1
SPE10 36, linear flux	40586	1835	34	2
SPE10 36, nonlinear flux	118364	7644	25	2

Numerical results

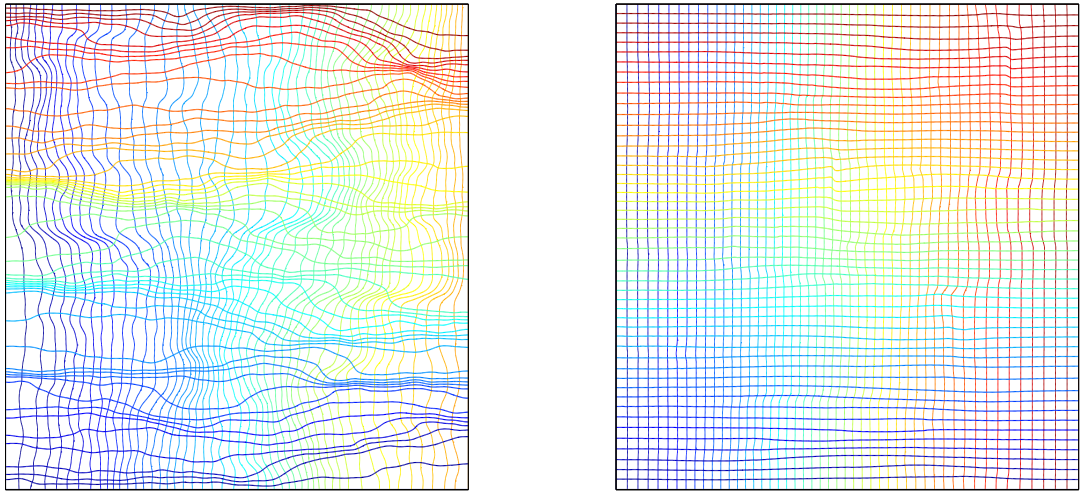

Left: Pressure and streamline function at time $t = 0.4$ in Cartesian frame. Right: pressure and streamline function at time $t = 0.4$ in initial pressure-streamline frame.
For two-phase flow, equations are upscaled on flow-based coordinate system. MsFEM using limited global information is equivalent to standard MsFEM.

Numerical results

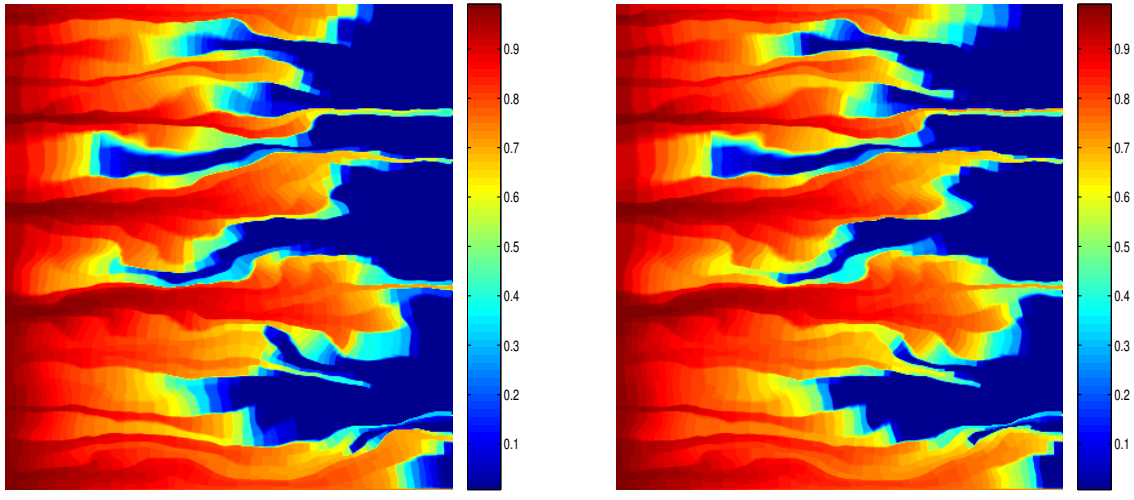

Left: Saturation plot obtained using coarse-scale model. Right: The fine-scale saturation plot. Both plots are on coarse grid. Variogram based permeability field is used. $\mu_o/\mu_w = 5$.

Numerical results

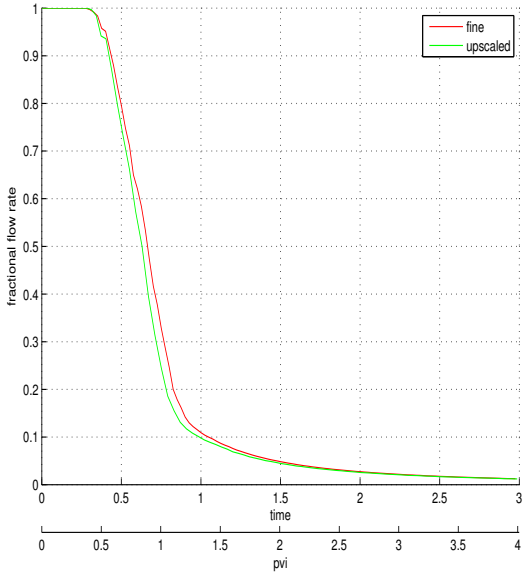

Comparison of fractional flow for coarse- and fine-scale models. Variogram based permeability field is used. $\mu_o/\mu_w = 5$.

Numerical results

Convergence of the upscaling method for two-phase flow for variogram based permeability

with $\tilde{S}$	50x50	100x100	200x200
L_2 pressure error at $t = \frac{3T_{final}}{4}$	0.0014	0.007	0.004
L_2 velocity error at $t = \frac{3T_{final}}{4}$	0.0235	0.0137	0.0072
L_1 saturation error $t = T_{final}$	0.0105	0.0052	0.0027

with $\overline{S}$	50x50	100x100	200x200
L_2 pressure error at $t = \frac{3T_{final}}{4}$	0.0046	0.0021	0.0008
L_2 velocity error at $t = \frac{3T_{final}}{4}$	0.0530	0.0335	0.0246
L_1 saturation error $t = T_{final}$	0.0546	0.0294	0.0134

Adaptive subgrid capturing algorithm for transport equation

Adaptive Multiscale Algorithm

For each $T \in \mathcal{T}^n_{\text{tr}}$, do

- For $K_i \subset T^E$, compute

$$S_i^{n+1/2} = S_i^n + \frac{\triangle t}{\int_{K_i} \phi \, dx} \left[\int_{K_i} q_w(S^{n+1/2}) - \sum_{j \neq i} V_{ij}^* \right],$$

where $V_{ij}^* = \begin{cases} V_{ij}(S^n) & \text{if } \gamma_{ij} \subset \partial T^E \text{ and } v_{ij} < 0. \\ V_{ij}(S^{n+1/2}) & \text{otherwise.} \end{cases}$

- Set $S^{n+1}|_T = S^{n+1/2}|_T$.

For each $T \notin \mathcal{T}^n_{\text{tr}}$, do

- Set $S^{n+1}|_T = S^n|_T$.
- While $\sum_j \triangle_j t \leq \triangle t$, compute

$$\bar{S}_T^{n+1} = \bar{S}_T^{n+1} + \frac{\triangle_j t}{\int_T \phi \, dx} \left[\int_T q_w(S^{n+1}) \, dx - \sum_{\gamma_{ij} \subset \partial T} V_{ij}(S^{n+1}) \right],$$

and set $S^{n+1}|_T = I_T(\bar{S}_T^{n+1})$.

Multiscale interpolation

The basis functions $\Phi_i^k = \chi_i(x, \tau_k)$ represent snapshots of the solution of the following equation:

$$\phi \frac{\partial \chi_i}{\partial t} + \nabla \cdot (f_w(\chi_i)v) = q_w \quad \text{in } T_i.$$

The multiscale interpolation is chosen as

$$I_{T_i}(\bar{S}_i^n) = \omega \Phi_i^k + (1-\omega)\Phi_i^{k+1},$$

where $\omega \in [0,1]$ is chosen such that the interpolation preserves mass, i.e., such that

$$\int_{T_i} I_{T_i}(\bar{S}_i^n)\phi \, dx = \bar{S}_i^n \int_{T_i} \phi \, dx.$$

Boundary condition on inflow boundaries?
Relation to extension of MsFEM to nonlinear problems.

The relation to pseudo type of approaches

$$\frac{\partial \overline{S}}{\partial t} + \nabla \cdot F^*(x, \overline{S}) = 0,$$

where $F^*(x, \overline{S}) = \overline{v} f_w^*$, $\overline{v}$ is the upscaled velocity field.
The pseudofunctions are computed from local fine scale problems such that they provide the same average response as the fine grid model for the prescribed boundary conditions. Assuming that the pseudofunctions have been computed, the corresponding coarse scale equation takes the following form:

$$\overline{S}^{n+1} = \overline{S}^n + \frac{\Delta t}{\int_T \phi dx} \left[\int_T q_w(S^n) dx - \sum_{\Gamma_{ij} \subset \partial T} V_{ij}^*(S^n) \right],$$

where $V_{ij}^*(S) = \max\{\overline{v}_{ij} f_{w,i}^*(\overline{S}_i), -\overline{v}_{ij} f_{w,j}^*(\overline{S}_j)\}$.
Advantages: (1) adaptivity; (2) ability to downscale; (3) avoid no flow boundaries.

Analysis

$$
\begin{aligned}
G_f(S) &= -\frac{1}{\int_T \phi\, dx} \int_{\partial T} f_w(S)(v \cdot n)\, ds, \\
G_c(\overline{S}) &= -\frac{1}{\int_T \phi\, dx} \int_{\partial T} f_w(I(\overline{S}))(v \cdot n)\, ds.
\end{aligned}
$$

Let

$$\delta^n = \overline{S}^n - \overline{S}_h^n.$$

It can be shown that

$$
|\delta^n| \leq o(\Delta t) + \Delta t \sum_{k=0}^{n-1} (1 + C\Delta t)^k |G_f(S^{n-k}) - G_c(\overline{S}^{n-k})| \leq o(\Delta t) + \left[\frac{e^{C(n\Delta t)} - 1}{C}\right] \left[\max_{1 \leq i \leq n} |G_f(S^i) - G_c(\overline{S}^i)|\right].
$$

If we assume scale separation, then $G_f(S) \approx G_c(\overline{S})$.

Analysis. Flow based coord. sys.

Assume $v_{tp} \approx A^*(x,t)v_{sp}$. where A^* is a scalar coarse-scale function. This assumption holds if streamlines do not change dramatically.
Denote by τ time-of-flight for single-phase flow velocity, $v_{sp} \cdot \nabla\tau = 1$. Then, the two-phase flow saturation equation has the form

$$\phi\frac{\partial S}{\partial t} + A^*(\tau,\psi,t)f(S)_\tau = 0,$$

where $A^*(\tau,\psi,t)$ denotes $A^*(x,t)$ in (τ,ψ) coordinate system. Assuming A^* is a bounded smooth function, the equation suggests that S is a smooth function along the lines $\tau = const$. Writing $G_f(S) \approx G_c(\overline{S})$ in (τ,ψ) coordinate system, we have

$$\int_{T_{\tau,\psi}} f_w(S)_\tau dV \approx \int_{T_{\tau,\psi}} f_w(I(\overline{S}))_\tau dV,$$

where $T_{\tau,\psi}$ is an image of T in (τ,ψ) coordinate system. Note that S and $I(\overline{S})$ satisfy $\phi\frac{\partial S}{\partial t} + A^*(\tau,\psi,t)f(S)_\tau = 0$ and $\phi\frac{\partial I(\overline{S})}{\partial t} + f(I(\overline{S}))_\tau = 0$, respectively.
$S = 1$ boundary condition overestimates the flow at the inlet of coarse blocks, especially in regions where τ varies significantly along the inlet boundary.

Alternatively, one can use extended domains with boundaries given by $\tau = const$ and $\psi = const$ for computation of basis functions in Cartesian coarse blocks. This reduces the error associated with saturation distribution across the streamlines in the coarse block.
Error at the inlet (1-D).

Numerical results

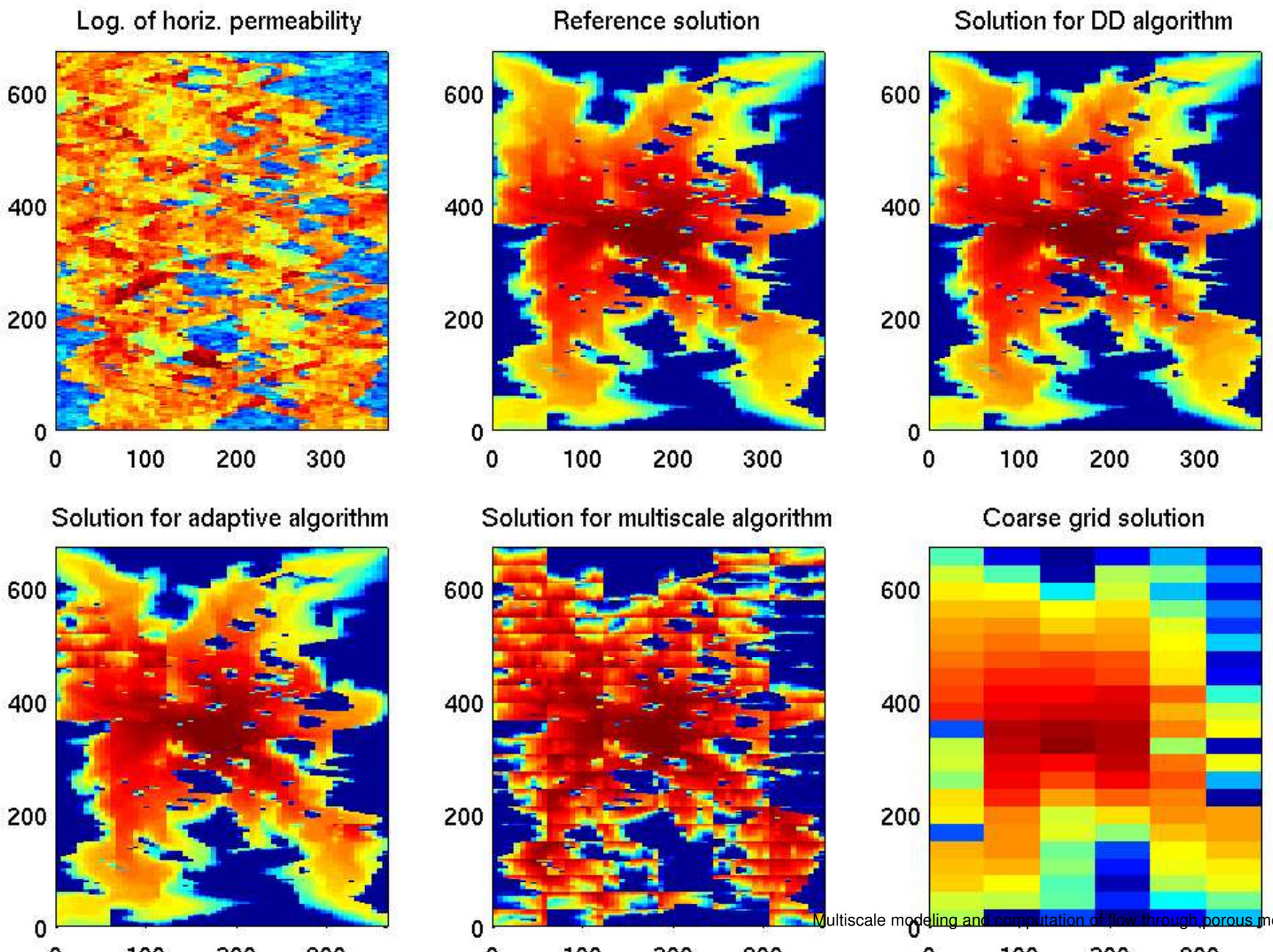

Numerical results

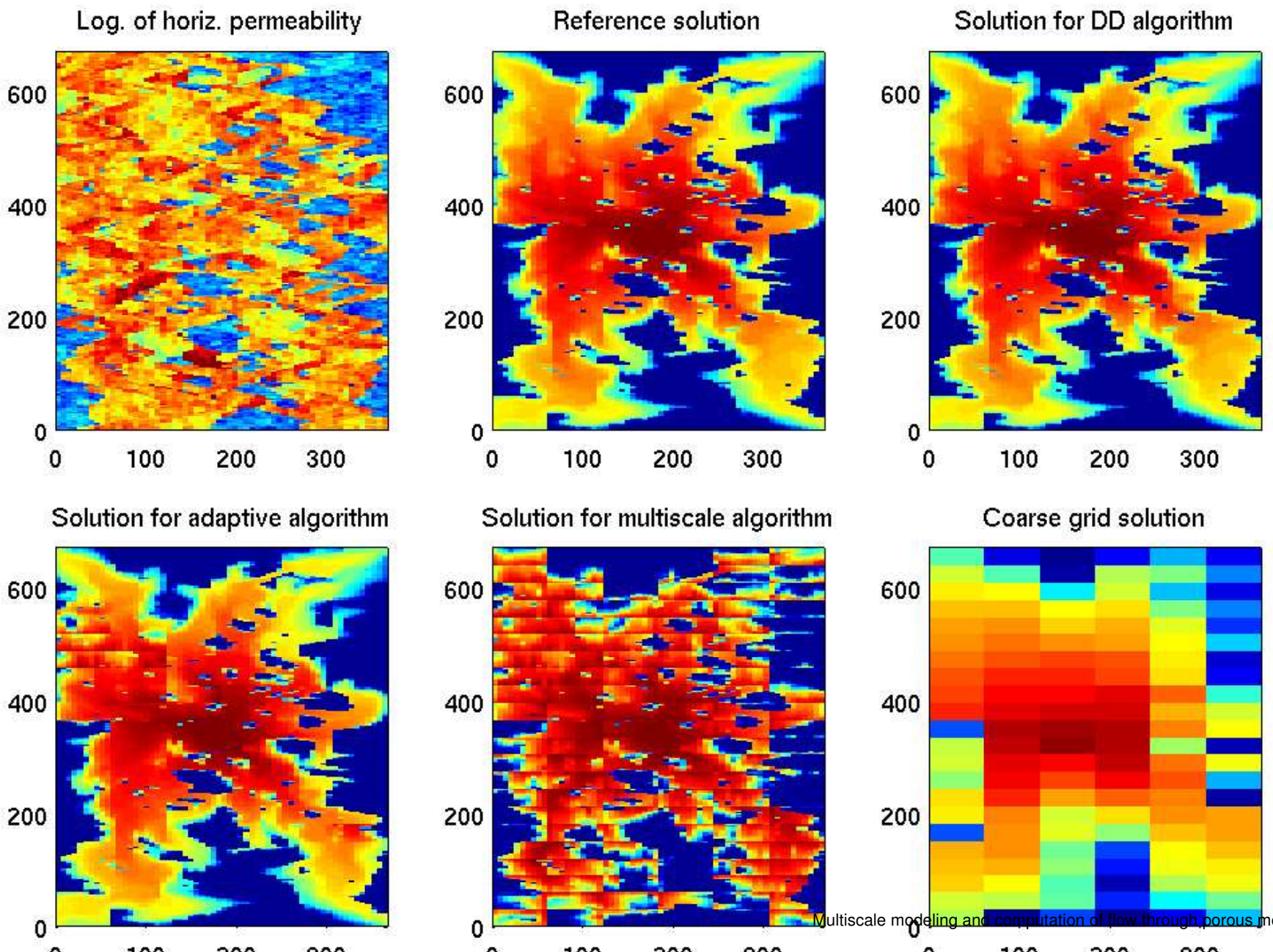

Numerical results

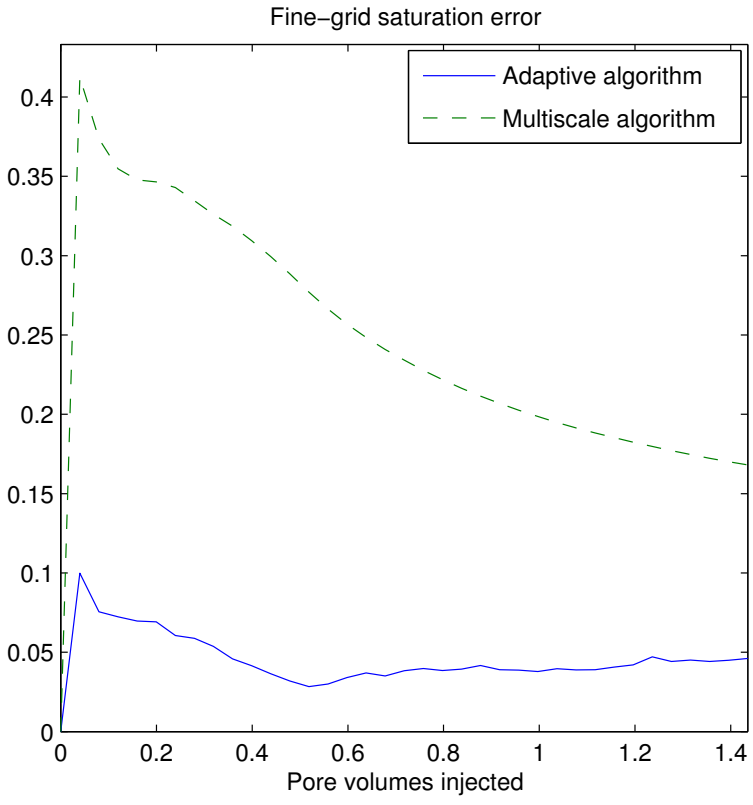

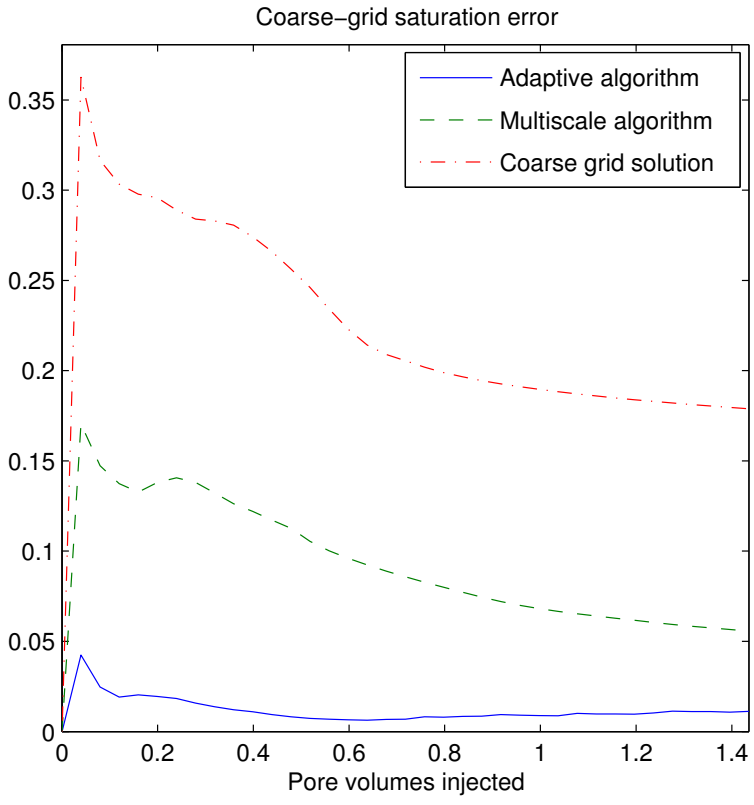

Numerical results

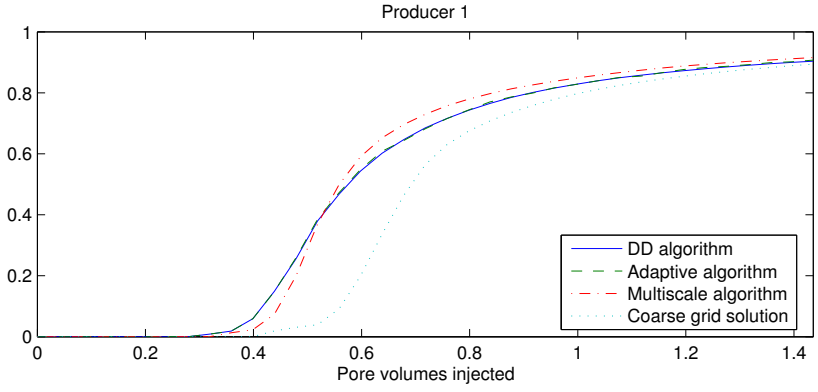

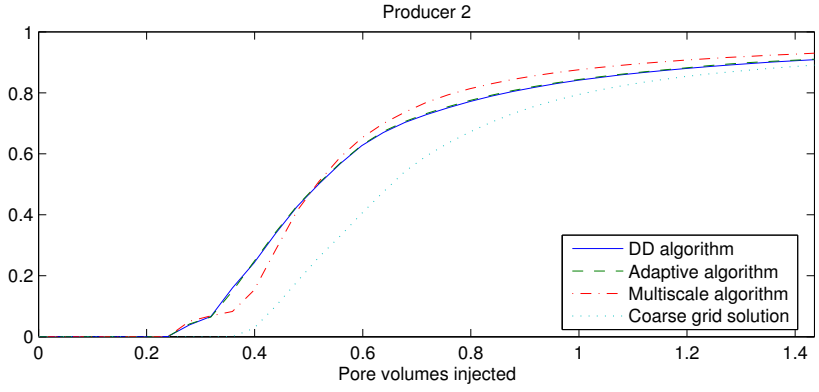

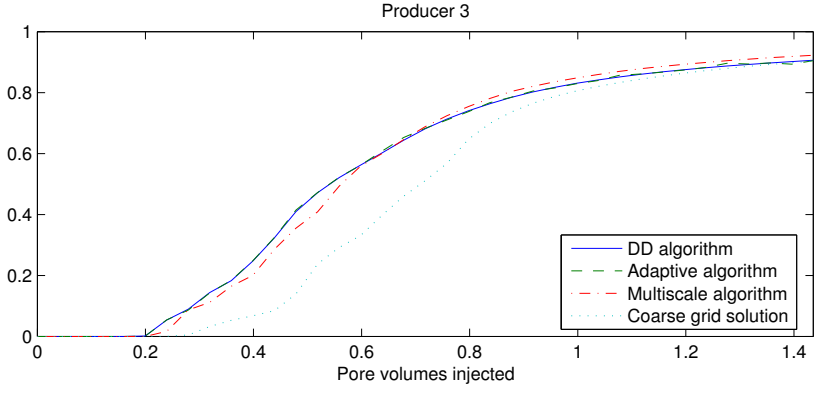

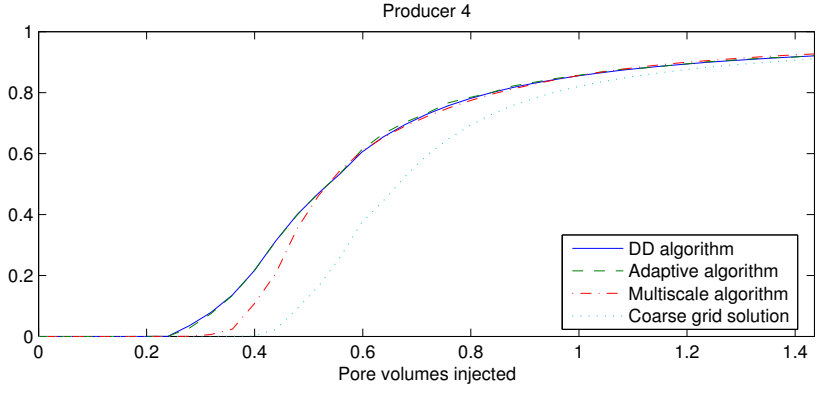

Applications of multiscale finite element methods to uncertainty quantification in porous media flows

Introduction

- Dynamic data integration in petroleum applications consists of integrating production data in order to reduce uncertainty and achieve realistic sampling of permeability field.
- Production data (usually measured with some precision) describes an integrated response (an average over the inter-well distance). Trying to obtain the permeability field samples based on this integrated response is an ill-posed problem.
- The problem reduces to sampling from a complicated distribition involving the solutions of coupled nonlinear partial differential equations.
- Metropolis-MCMC methods can be used for the sampling. One of the main difficulties is low acceptance rate.
- We propose and analyze approaches for increasing the acceptance rate using coarse-scale models.

Problem setting

Given the fractional flow information $F(t)$ and some precision, we would like to sample k. From Bayes' theorem

$$P(k|F) \propto P(F|k)P(k).$$

Here $P(k)$ is the prior information, $P(F|k)$ is the likelihood and assumed given by $P(F|k) = \exp(-\frac{\|F_k(t) - F^{obs}(t)\|^2}{\sigma_f^2})$.

The objective is the proper sampling from the complicated distribution $\pi(k) = P(k|F)$.

Difficulties

- $\pi(k) = P(k|F)$ is multi-modal.
- $\pi(k) = P(k|F)$ is not given analytically and involves the solution of nonlinear pde system.

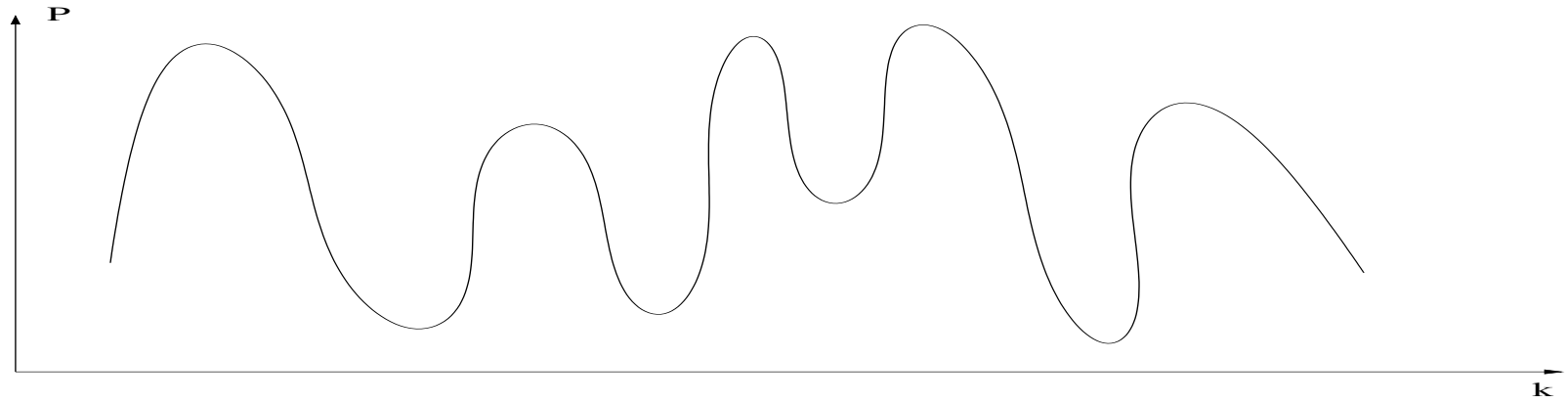

Figure 1:

Sampling using Metropolis-MCMC

Algorithm (Metropolis-Hasting MCMC)

- Step 1. At k_n generate k from $q(k|k_n)$.
- Step 2. Accept k as a sample with probability

$$p(k_n, k) = \min\left(1, \frac{q(k_n|k)\pi(k)}{q(k|k_n)\pi(k_n)}\right),$$

  i.e. $k_{n+1} = k$ with probability $p(k_n, k)$, and $k_{n+1} = k_n$ with probability $1 - p(k_n, k)$.

Here $\pi(k) = P(k|F)$. This process creates an ergodic Markov chain (under some general conditions) with the stationary distribution $\pi(k)$.

Sampling using Metropolis-MCMC

Algorithm (Metropolis-Hasting MCMC)

- Step 1. At k_n generate k from $q(k|k_n)$.
- Step 2. Accept k as a sample with probability

$$p(k_n, k) = \min\left(1, \frac{q(k_n|k)\pi(k)}{q(k|k_n)\pi(k_n)}\right),$$

i.e. $k_{n+1} = k$ with probability $p(k_n, k)$, and $k_{n+1} = k_n$ with probability $1 - p(k_n, k)$.

Here $\pi(k) = P(k|F)$. This process creates an ergodic Markov chain (under some general conditions) with the stationary distribution $\pi(k)$.
Discrete setting (state space: $1, .., n$)
(1) At each i, propose j, using q_{ij}.
(2) Accept j with probability $\frac{\pi_j q_{ji}}{\pi_i q_{ij}}$.

Metropolis-Hasting rule

- Direct (full) MCMC simulations are usually prohibitively expensive, because each proposal requires a fine-scale computation.
- Direct MCMC usually requires many (thousand) of iterations for the convergence to a steady state, where each iteration involves the computation of the fine-scale solution over a large time interval.
- The acceptance rate of direct MCMC is usually small, i.e., most proposals will be rejected.
- One way to improve direct MCMC is to increase the acceptance rate by modifying the proposal. We propose an algorithm, where the proposal distribution is modified using coarse-scale model.

Typical fine and coarse results

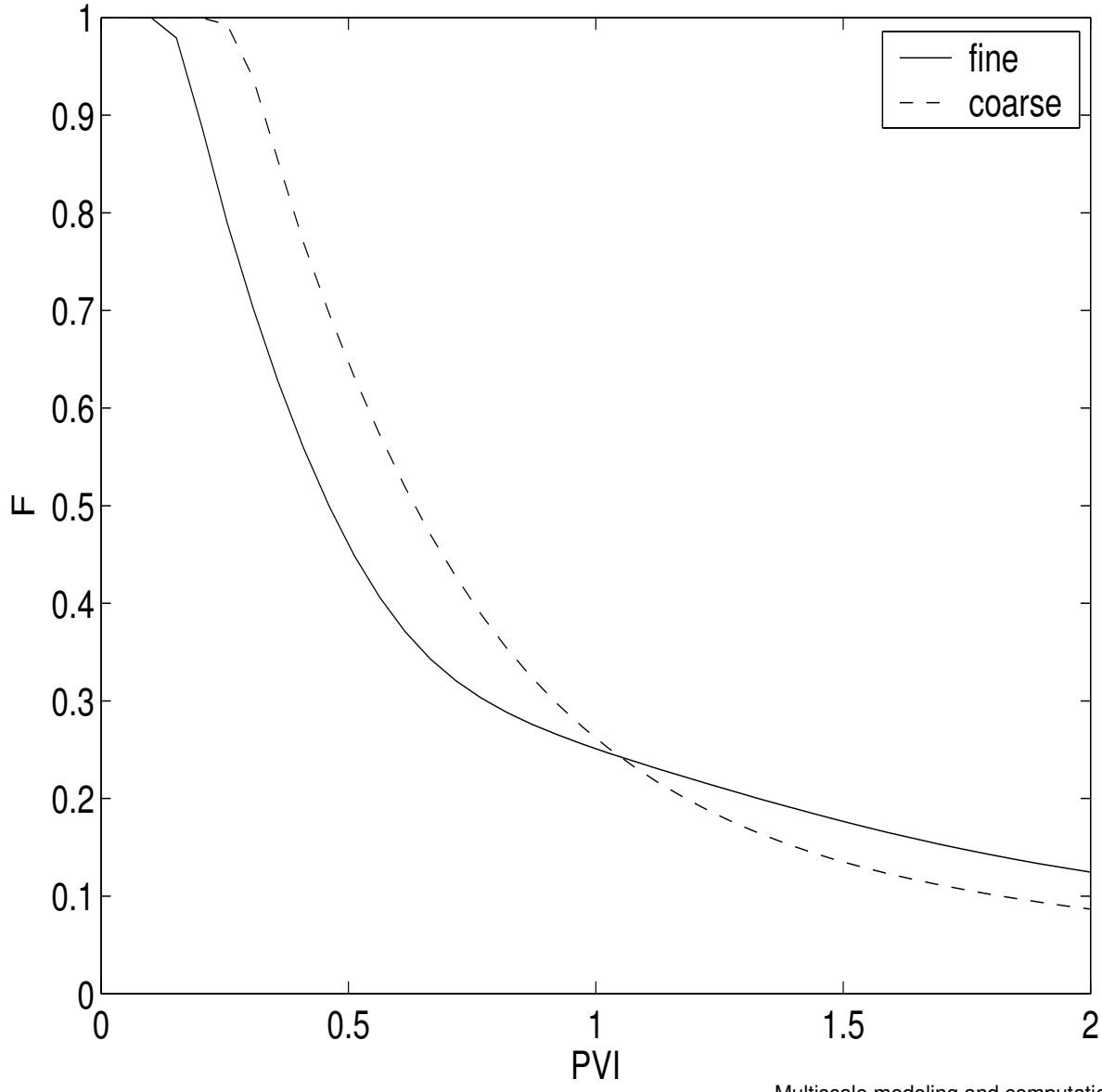

Remark

Coarse-scale posterior is smoother and do not have all local maxima of fine-scale posterior

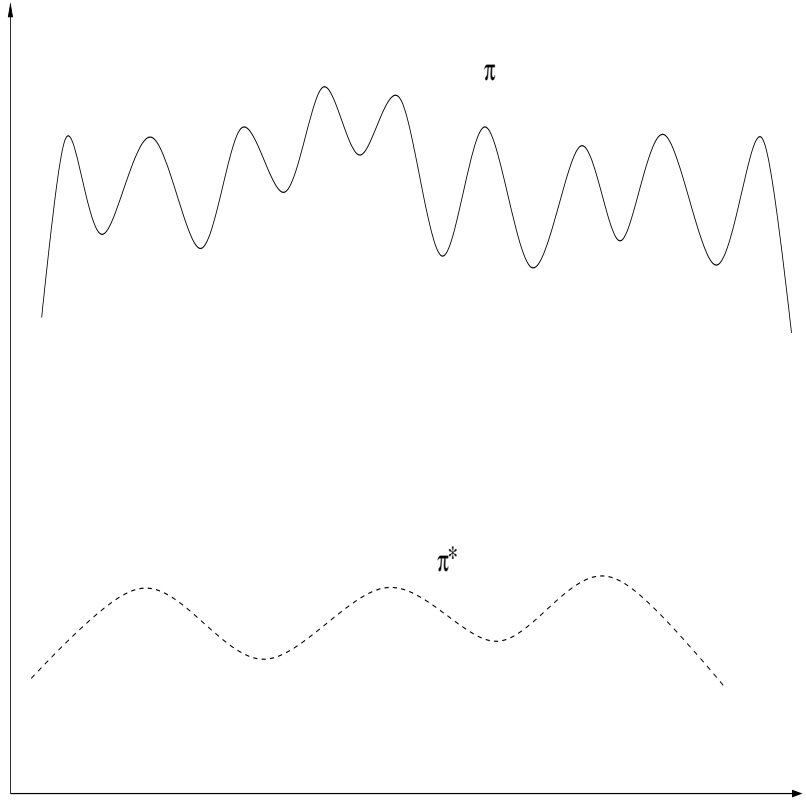

Response surfaces

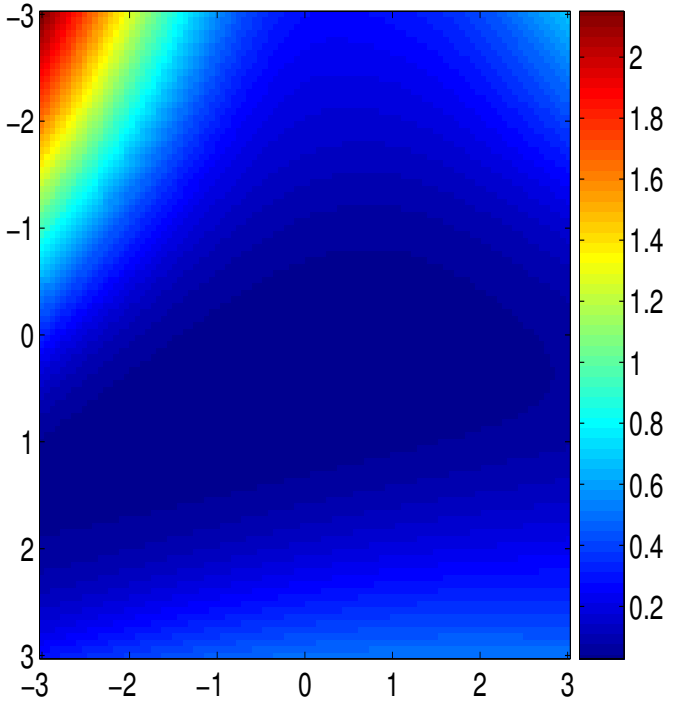

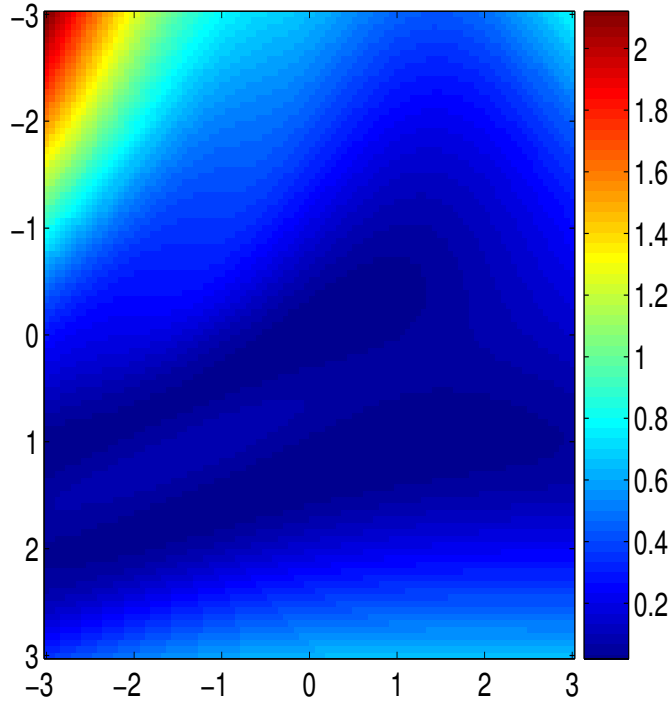

Preconditioning of MCMC

Algorithm (preconditioned MCMC)

- Step 1. At k_n, generate k from distribution $q(k|k_n)$.
- Step 2. Accept k as a proposal for *the fine-scale model* with probability

$$g(k_n, k) = \min\left(1, \frac{q(k_n|k)\pi^*(k)}{q(k|k_n)\pi^*(k_n)}\right),$$

i.e. pass k or k_n as a proposal to the fine-scale model with probability $g(k_n, k)$ or $1 - g(k_n, k)$ respectively. Here $\pi^*(k) = P(k^*|F)$. Therefore, the final proposal to the fine-scale model is generated from the effective instrument distribution

$$Q(k|k_n) = g(k_n, k)q(k|k_n) + \left(1 - \int g(k_n, k)q(k|k_n)dk\right)\delta_{k_n}(k).$$

- Step 3. Accept k as a sample with probability

$$\rho(k_n, k) = \min\left(1, \frac{Q(k_n|k)\pi(k)}{Q(k|k_n)\pi(k_n)}\right),$$

i.e. $k_{n+1} = k$ with probability $\rho(k_n, k)$, and $k_{n+1} = k_n$ with probability $1 - \rho(k_n, k)$.

Convergence of modified Markov Chain

First it can be shown that

$$\rho(k_n, k) = \min\left(1, \frac{\pi(k)\pi^*(k_n)}{\pi(k_n)\pi^*(k)}\right).$$

Denote

$$\mathcal{E} = \{k;\ \pi(k) > [0]\},$$
$$\mathcal{E}^* = \{k;\ \pi^*(k) > [0]\},$$
$$\mathcal{D} = \{k;\ q(k|k_n) > [0] \text{ for some } k_n \in \mathcal{E}\},$$

To sample from $\pi(k)$ correctly, it is necessary that $\mathcal{E} \subseteq \mathcal{E}^*$. Otherwise, there will exist a subset $A \subset (\mathcal{E} \setminus \mathcal{E}^*)$ such that

$$\pi(A) = \int_A \pi(x)dx > 0 \qquad \text{and} \qquad \pi^*(A) = \int_A \pi^*(x)dx = 0.$$

As a result, the chain $\{k_n\}$ will never visit (sample from) A since the element of A will never be accepted for fine-scale run in Step 2. For the same reason, we should require that $\mathcal{E} \subseteq \Omega$.

Convergence of modified Markov Chain

The transition probability of the chain is defined by

$$K(k_n, k) = \rho(k_n, k)Q(k|k_n),\ k \neq k_n, \qquad \text{and} \qquad K(k_n, \{k_n\}) = 1 - \int_{k \neq k_n} \rho(k_n, k)Q(k|k_n)d$$

Lemma.

$$\pi(k_n)K(k_n, k) = \pi(k)K(k, k_n)$$

for any $k, k_n \in \mathcal{E}$.

Lemma. If the proposal $q(y|x)$ satisfies positivity condition, then the chain $\{k_n\}$ generated by the preconditioned MCMC method is strongly π-irreducible and aperiodic.

Theorem. Suppose proposal is positive, then the chain generated by the preconditioned MCMC method is ergodic: for any $h \in L^1(\pi)$,

$$\lim_{T \to \infty} \frac{1}{N} \sum_{n=1}^{N} h(k_n) = \int h(k)\pi(k)dk,$$

and the distribution of the chain $\{k_n\}$ converges to $\pi(k)$ in the total variation norm

$$\lim_{n \to \infty} \sup_{A} \left| K^n(k_0, A) - \pi(A) \right| = 0$$

Convergence of modified Markov Chain

$$P(F^*|k) \propto \exp\Big(-\frac{\|F^* - F_k^*\|^2}{\sigma_c^2}\Big).$$

Choosing Gaussian precisions we have

$$P(k_n, k) = \min\left(1, \frac{\pi(k)\pi^*(k_n)}{\pi(k_n)\pi^*(k)}\right) = \min\left(1, \exp\Big(-\frac{E_k - E_{k_n}}{\sigma_f^2}\Big)\exp\Big(\frac{E_k^* - E_{k_n}^*}{\sigma_c^2}\Big)\right)$$

where

$$E_k = \|F - F_k\|^2, \quad E_k^* = \|F^* - F_k^*\|^2.$$

Numerical setting. Parameterization

$k(x) = \exp(Y(x))$, where

$$Y(x,\omega) = \sum_{k=1}^{\infty} \sqrt{\lambda_k}\theta_k(\omega)\phi_k(x),$$

$E(\theta_k) = 0$ and $E(\theta_i\theta_j) = \delta_{ij}$.
We consider the Gaussian fields

$$R(x,y) = \sigma^2 \exp\left(-\frac{|x_1 - y_1|^2}{2L_1^2} - \frac{|x_2 - y_2|^2}{2L_2^2}\right).$$

The permeability field is conditioned at some locations.

$$\sum_{k=1}^{20} \sqrt{\lambda_k}\theta_k\phi_k(x_j) = \alpha_j,$$

Instrumental distribution

- Two type of instrumental proposal distribution, independent sampler and random walk sampler.
- In the case of independent sampler, the proposal distribution $q(k|k_n)$ is chosen to be independent of k_n and equal to the prior distribution.
- In random walk sampler, the proposal distribution depends on the previous value of the permeability field and given by

$$q(k|k_n) = k_n + \epsilon_n,$$

where ϵ_n is a random perturbation with prescribed variance.

Independent sampler

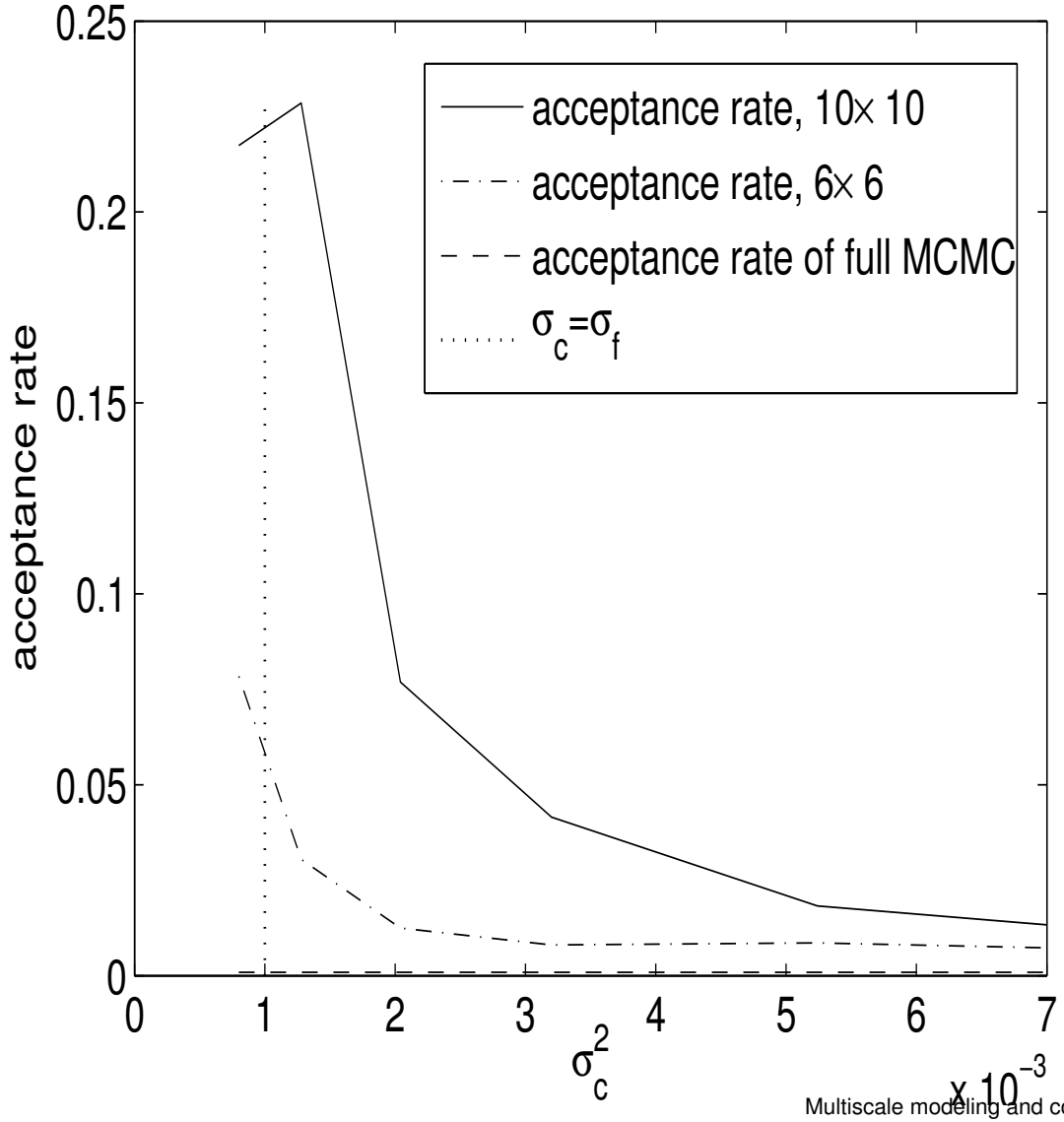

Brownian sampler

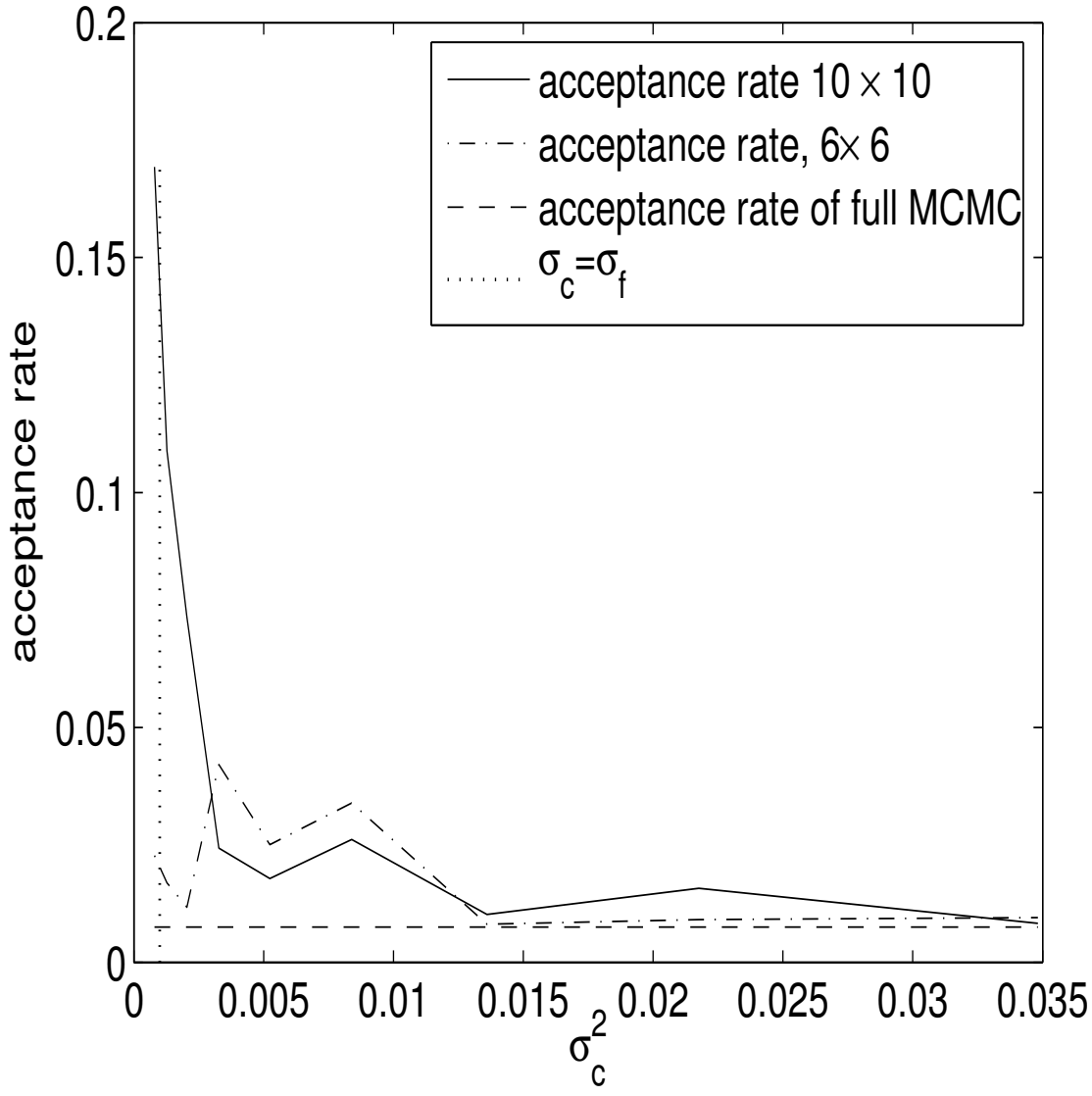

Langevin Algorithms

An important type of proposal distribution can be derived from the Langevin diffusion. The Langevin diffusion is defined by the stochastic differential equation

$$dk(\tau) = \frac{1}{2}\nabla \log \pi(k(\tau))d\tau + dW_\tau,$$

where W_τ is the standard Brownian motion vector with independent components. A discretization of the equation,

$$k_{n+1} = k_n + \frac{\Delta\tau}{2}\nabla \log \pi(k_n) + \sqrt{\Delta\tau}\epsilon_n,$$

where ϵ_n are independent standard normal distributions. The proposal is chosen to be

$$Y = k_n + \frac{\Delta\tau}{2}\nabla \log \pi(k_n) + \sqrt{\Delta\tau}\epsilon_n,$$

Langevin Algorithms

The transition distribution of the proposal is

$$q(Y|k_n) \propto \exp\left(-\frac{\|Y - k_n - \frac{\Delta\tau}{2}\nabla \log \pi(k_n)\|^2}{2\Delta\tau}\right),$$

$$q(k_n|Y) \propto \exp\left(-\frac{\|k_n - Y - \frac{\Delta\tau}{2}\nabla \log \pi(Y)\|^2}{2\Delta\tau}\right).$$

The use of the gradient information in inverse problems for subsurface characterization - RML (by Oliver et al.).
This approach uses unconditional realizations of the production and permeability data and solves a deterministic gradient-based minimization problem.

Preconditioned coarse-gradient Langevin algorithm

- Step 1. At k_n, generate a trial proposal Y from the coarse Langevin distribution $q^*(Y|k_n)$.
- Step 2. Take the proposal k as

$$k = \begin{cases} Y \text{ with probability } g(k_n, Y), \\ k_n \text{ with probability } 1 - g(k_n, Y), \end{cases}$$

where

$$g(k_n, Y) = \min\left(1, \frac{q^*(k_n|Y)\pi^*(Y)}{q^*(Y|k_n)\pi^*(k_n)}\right).$$

Therefore, the proposal k is generated from the effective instrumental distribution

$$Q(k|k_n) = g(k_n, k)q^*(k|k_n) + \left(1 - \int g(k_n, k)q^*(k|k_n)dk\right)\delta_{k_n}(k).$$

- Step 3. Accept k as a sample with probability

$$\rho(k_n, k) = \min\left(1, \frac{Q(k_n|k)\pi(k)}{Q(k|k_n)\pi(k_n)}\right),$$

Preconditioned coarse-gradient Langevin algorithm

The transition distribution of the coarse-grid proposal is

$$q^*(Y|k_n) \propto \exp\left(-\frac{\|Y - k_n - \frac{\Delta\tau}{2}\nabla \log \pi^*(k_n)\|^2}{2\Delta\tau}\right),$$

$$q^*(k_n|Y) \propto \exp\left(-\frac{\|k_n - Y - \frac{\Delta\tau}{2}\nabla \log \pi^*(Y)\|^2}{2\Delta\tau}\right).$$

We have proved that the modified Markov chain is ergodic and samples from the correct posterior.

Numerical results

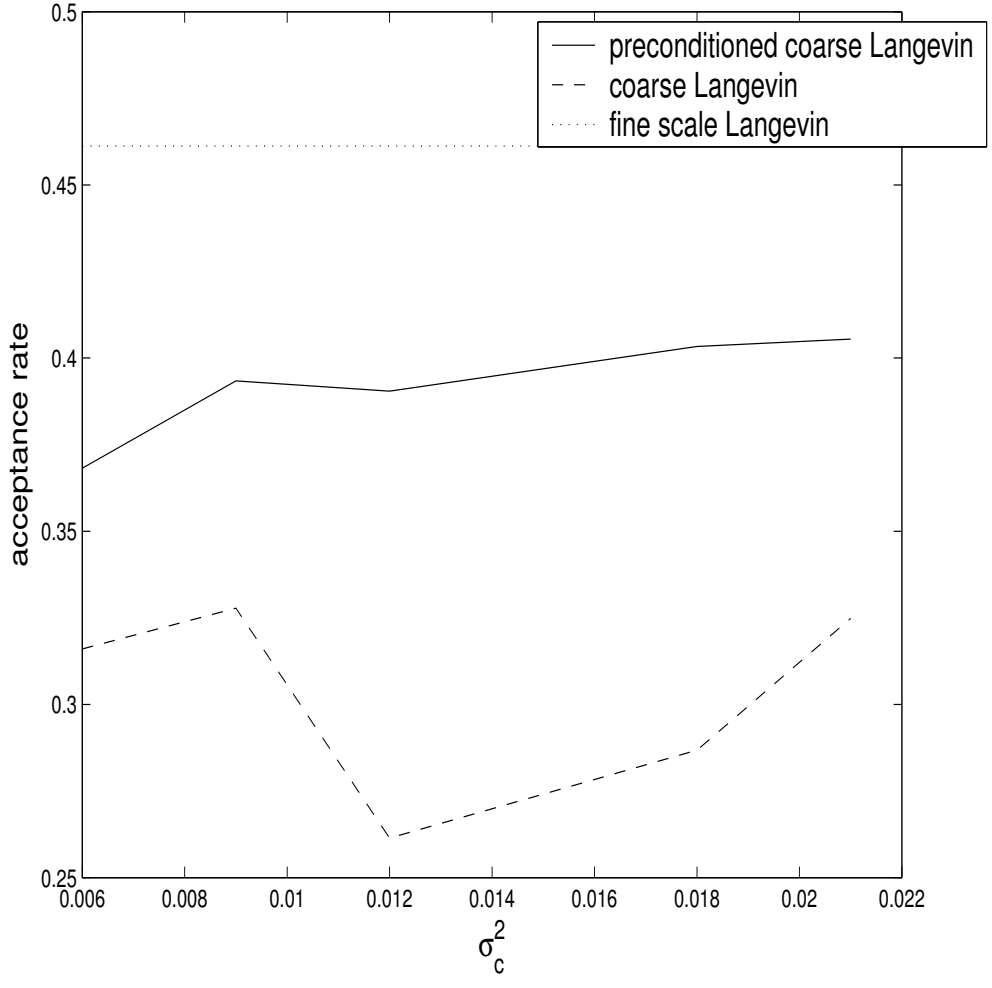

Acceptance rate comparison, $\delta = 0.1$.

Numerical results

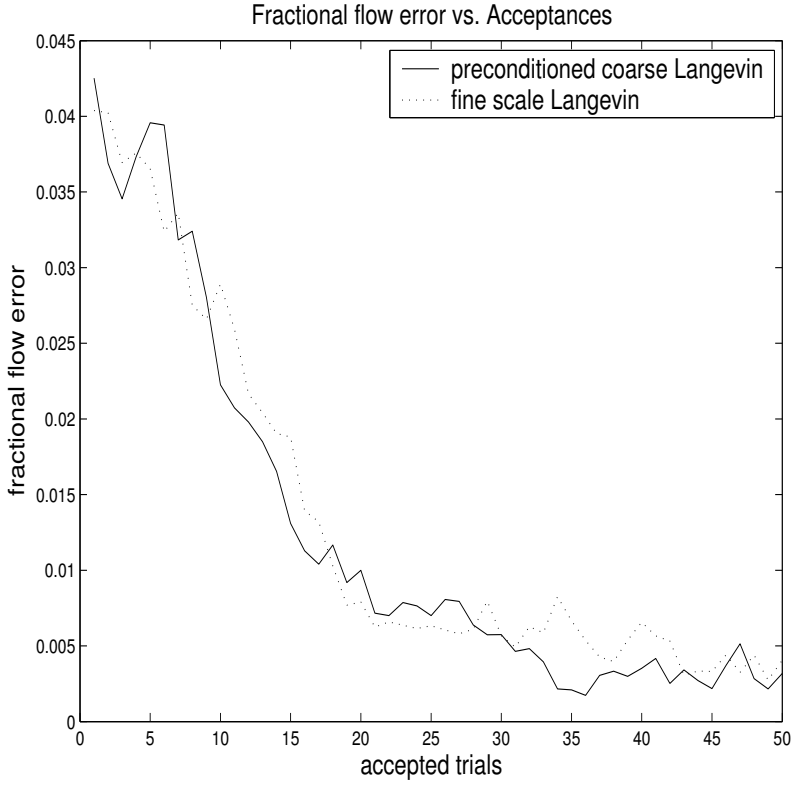

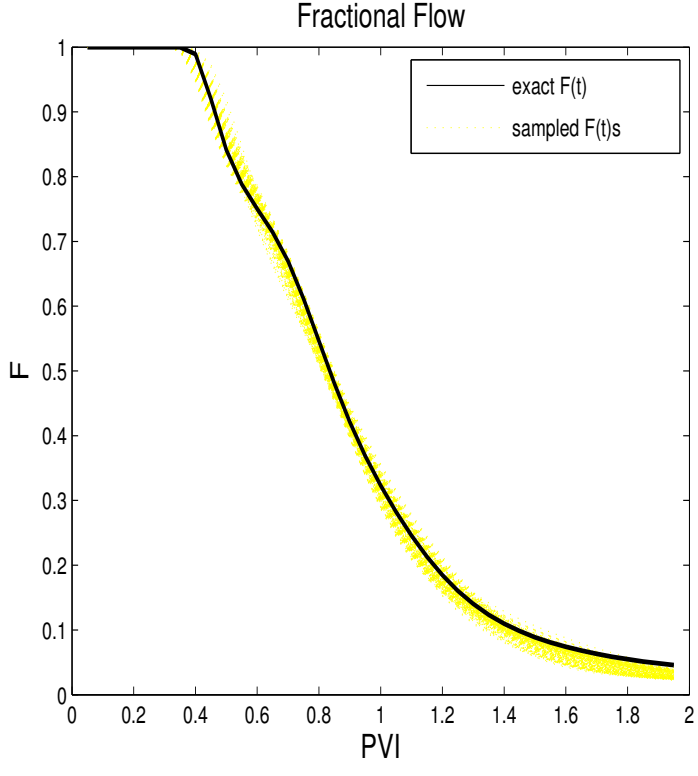

Numerical results

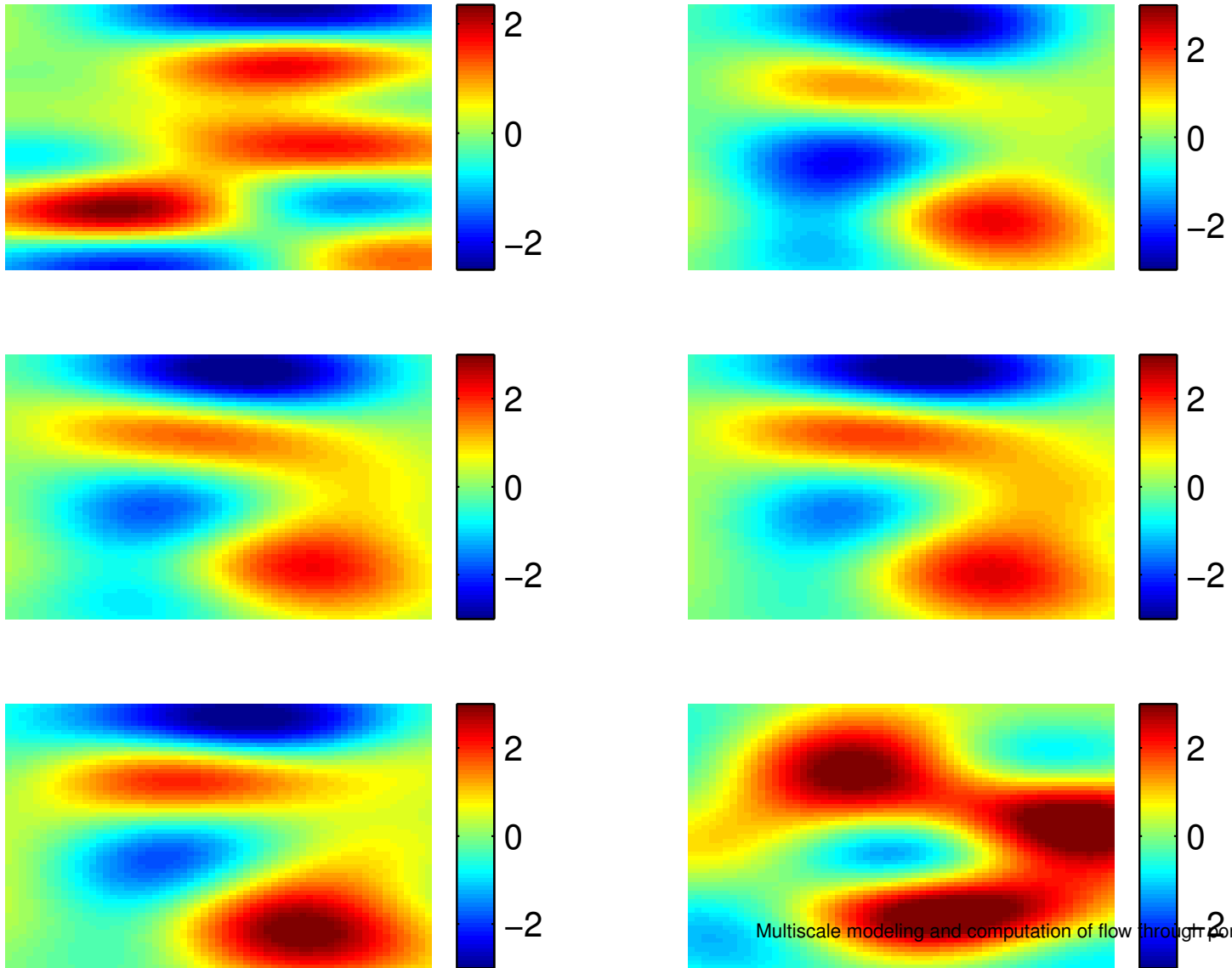

Numerical results

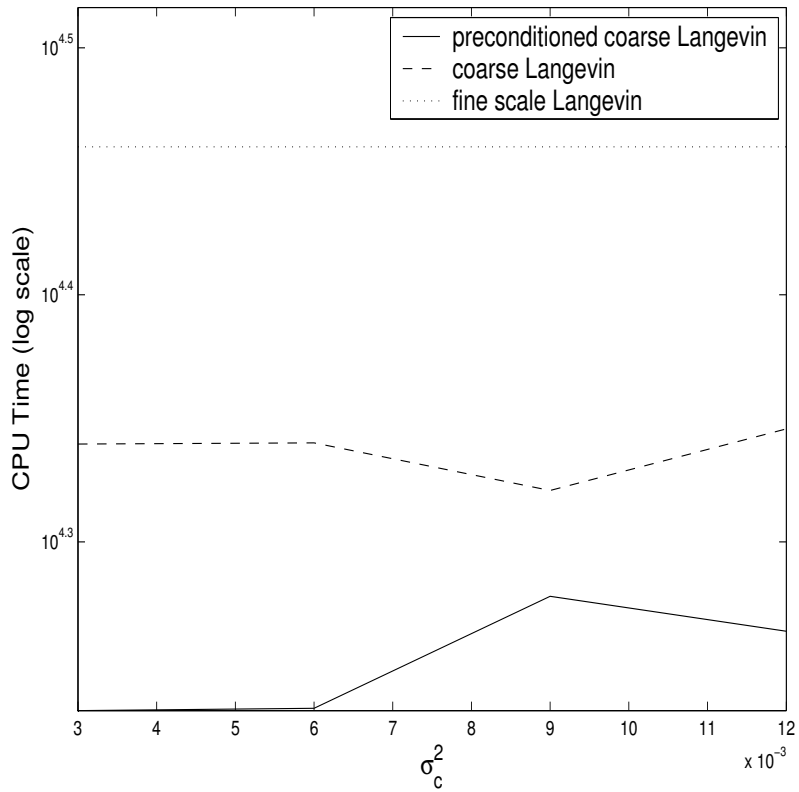

Numerical results

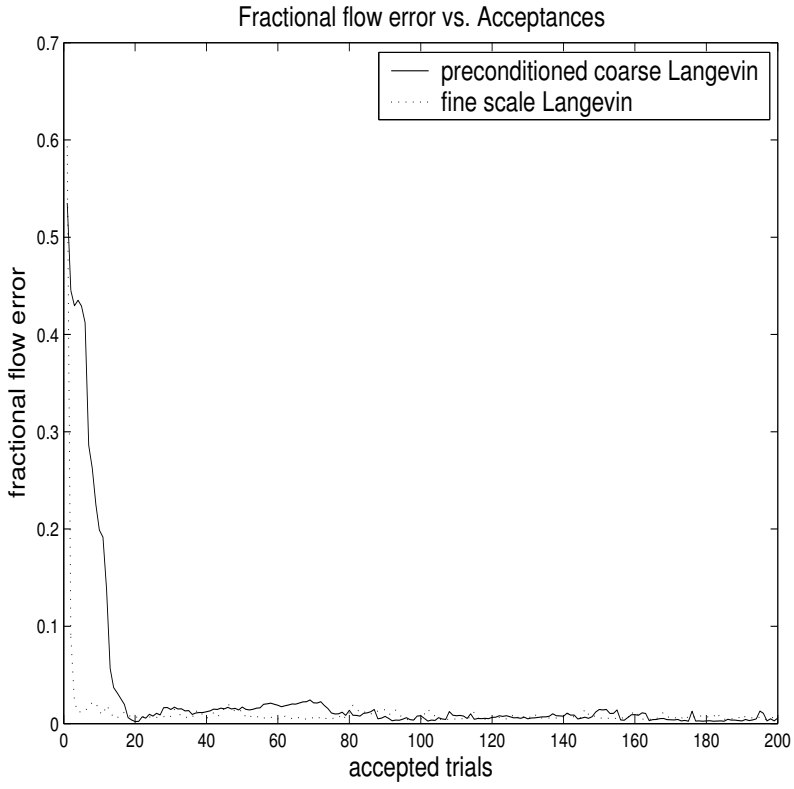

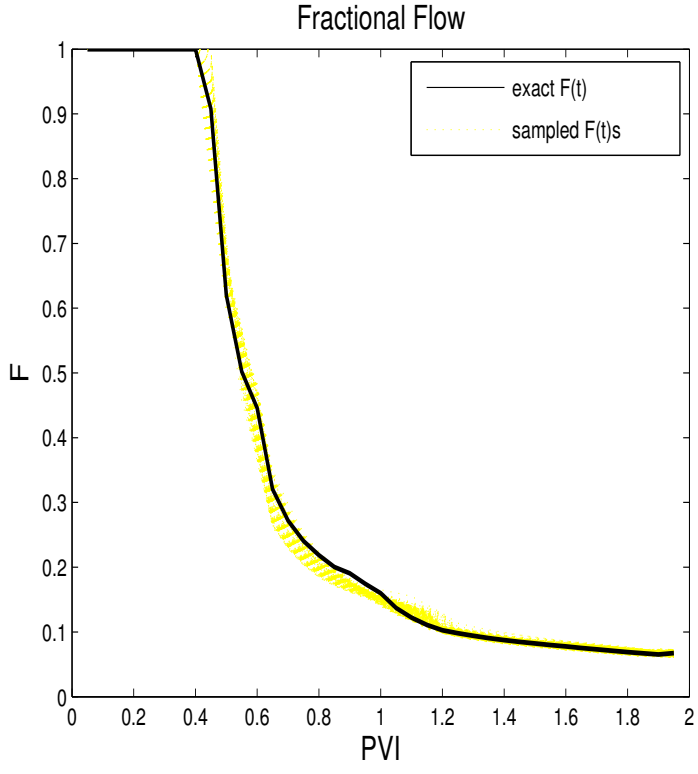

Numerical results